ORDER RECONSTRUCTION FOR NEMATICS ON SQUARES AND HEXAGONS: A LANDAU-DE GENNES STUDY

GIACOMO CANEVARI, APALA MAJUMDAR & AMY SPICER

Abstract. We construct an order reconstruction (OR)-type Landau-de Gennes critical point on a square domain of edge length 2λ, motivated by the well order reconstruction solution numerically reported in [1]. The OR critical point is distinguished by an uniaxial cross with negative scalar order parameter along the square diagonals. The OR critical point is defined in terms of a saddle-type critical point of an associated scalar variational problem. The OR-type critical point is globally stable for small λ and undergoes a supercritical pitchfork bifurcation in the associated scalar variational setting. We consider generalizations of the OR-type critical point to a regular hexagon, accompanied by numerical estimates of stability criteria of such critical points on both a square and a hexagon in terms of material-dependent constants.

1. Introduction. Nematic liquid crystals (LCs) are anisotropic liquids or liquids with a degree of long-range orientational order [2, 3]. Nematics in confinement offer ample scope for pattern formation and scientists are keen to better understand and exploit pattern formation to design new LC-based devices with advanced optical, mechanical and even rheological properties. This paper is motivated by the well order-reconstruction solution for square wells, numerically reported in [1], and its potential generalizations to other symmetric geometries.

Nematic-filled square or rectangular wells have been widely studied in the literature [4, 5, 6, 7]. In [4], the authors study the planar bistable device comprising a periodic array of micron-scale shallow nematic-filled square or rectangular wells. The well surfaces were treated to induce tangent or planar boundary conditions so that the well molecules in contact with these surfaces are constrained to be in the plane of the surfaces. In the absence of any external fields, the authors observe at least two different static equilibria: the diagonal state for which the molecules roughly align along one of the square diagonals and the rotated state for which the molecules roughly rotate by π radians between a pair of opposite edges.

In [1], the authors numerically model this device within the Landau-de Gennes (LdG) theory for nematic LCs. The LdG theory describes the nematic state by a symmetric, traceless 3×3 matrix — the $\mathbf{Q}$-tensor order parameter that is described in Section 2 below. In [1], the authors study static equilibria in the LdG framework, on a square domain with tangent boundary conditions. For square dimensions much larger than a material and temperature-dependent length scale known as the biaxial correlation length, the authors recover the familiar diagonal and rotated solutions. For squares with edge length comparable to the biaxial correlation length, the authors find a new well order reconstruction solution (WORS) for which the LdG $\mathbf{Q}$-tensor has a constant set of eigenvectors, one of which is $\hat{\mathbf{z}}$ — the unit vector in the z-direction. The WORS has a "uniaxial" diagonal cross along which the LdG $\mathbf{Q}$-tensor has two equal positive eigenvalues (so that the non-degenerate eigenvalue is negative and the cross has negative order parameter), surrounded by a ring of "maximal biaxiality" for which the LdG $\mathbf{Q}$-tensor has a zero eigenvalue, matched by Dirichlet conditions on the square edges. The WORS is interesting because it is a two-dimensional example of an order reconstruction solution on a square i.e. the LdG $\mathbf{Q}$-tensor mediates between the diagonal cross connecting the four vertices and the Dirichlet edge conditions without any distortion of the eigenframe but by sheer variations in the eigenvalues of the LdG $\mathbf{Q}$-tensor, referred to as *eigenvalue exchange* in the literature. From an

applications point of view, it can potentially offer very different optical properties to the conventional diagonal and rotated solutions should it be experimentally realized. Further, for squares with edge length less than a certain material-dependent and temperature-dependent critical length, the WORS appears to be the unique (stable) LdG equilibrium, as suggested by the numerics in [1].

Order reconstruction (OR) solutions have a long history in the context of nematic LCs. They were reported in [8, 9, 10] for nematic defect cores where the defect core is surrounded by a torus of maximal biaxiality; the torus mediates between or connects the nematic state at the defect core with the configuration away from the core. OR solutions were successfully studied for hybrid nematic cells, typically consisting of a layer of nematic material sandwiched between a pair of parallel plates, each of which has a preferred boundary orientation for the nematic molecules [11, 12, 13]. In [11], the authors consider the case of mutually orthogonal boundary conditions. For small cell gaps, the authors find an OR solution with a constant eigenframe that connects the two conflicting boundary alignments through one-dimensional eigenvalue variations across the normal to the plates. Indeed, the OR solution is the only observable solution (and hence globally stable) for cell gaps smaller than a certain critical value. For larger cell gaps, the authors observe familiar twisted profiles for which the eigenvectors rotate continuously throughout the cell to match the boundary alignments. The authors numerically compute a bifurcation diagram and show that the OR solution undergoes a supercritical pitchfork bifurcation to the familiar twisted solutions at a critical cell gap. In [14], the author rigorously studies the hybrid cell in a one-dimensional variational setting, in the LdG framework, and rigorously proves the existence of an OR solution, uniqueness for small cell gaps, and the supercritical pitchfork bifurcation as the cell gap increases, at least for a range of temperatures. In [12], the authors consider the hybrid cell problem for non-orthogonal boundary conditions. Their findings are contrasting to those of [11] in the sense that they find an unstable OR solution for cell gaps larger than a critical value and the familiar twisted solutions are always preferred irrespective of cell gap. In a similar vein, OR solutions have also been numerically reported in cylindrical tubes with an annular cross-section in [15] recently where the authors investigate OR patterns as a function of the cylindrical aspect ratio and other model parameters.

We provide a semi-analytic description of the numerically discovered WORS, and study its stability properties as a function of square size, measured by λ. We work in the LdG framework and impose Dirichlet tangent conditions on the edges, consistent with the experiments reported in [4], but there is a natural mismatch at the vertices. We truncate the vertices and hence, study a Dirichlet boundary-value problem on a truncated square, with four long edges that are common to the original square and four short edges that are straight lines connecting the long edges. We conjecture that the artificial short edges do not change the qualitative conclusions of our work, as is corroborated by the numerics in Section 6.

We work at a fixed temperature below the nematic supercooling temperature, largely for analytic convenience, and the fixed temperature only depends on material-dependent constants (see Sections 2 and 3 below). This fixed temperature is identical to the fixed temperature used in [14], Section 5 in the one-dimensional context. We search for LdG equilibria that can mimic the numerically observed WORS. We parameterize these critical points by three order parameters, q_1, q_2 and q_3, and the Dirichlet conditions translate into Dirichlet conditions for these variables. At the fixed temperature under consideration, we can prove the existence of a class of LdG critical points with

$q_2 = 0$ and constant q_3, with simply one degree of freedom labelled by q_1, for all values of λ. The vanishing q_2 guarantees a constant eigenframe and we think of q_1 as a measure of the in-plane alignment of the nematic molecules. The uniaxial cross is equivalent to $q_1 = 0$ along the square diagonals. We appeal to ideas from saddle solutions for bistable Allen-Cahn equations in [17, 18] to interpret q_1 as a minimizer of a scalar variational problem on a quadrant of a truncated square with Dirichlet conditions. We then define q_1 on the entire truncated square by an odd reflection of the quadrant solution across the diagonals, yielding a LdG critical point on the entire domain. This critical point has $q_1 = 0$ along the diagonals by construction, exists for all λ and reproduces the qualitative properties of the WORS. We refer to this LdG critical point as being the *OR* or *saddle-type* LdG critical point in the rest of the paper.

The OR LdG critical point is the unique critical point (and hence globally stable) for small λ, as can be demonstrated by a uniqueness argument used in [14]. Further, in Section 5, we prove that the OR LdG critical point, which can also be interpreted as a critical point of a scalar variational problem, undergoes a supercritical pitchfork bifurcation in the scalar setting as λ increases. In other words, it is unstable for large λ and hence, not observed for large micron-scale wells studied in [4, 6]. By carrying out a bifurcation analysis for a reduced scalar problem, we are able to prove rigorous results about the loss of stability of the WORS in the full LdG setting. The solution branches that appear past the bifurcation point in the scalar setting are also critical points of the LdG energy functional, but need not be stable in the full LdG framework; they are only stable in the reduced scalar setting. There are now detailed bifurcation plots for solutions in the full LdG framework [19], but we do not attempt to relate the numerical results for the full LdG problem with our bifurcation result in the scalar setting.

In Section 6, we study the gradient flow model for the LdG energy on a square with Dirichlet conditions and special OR-type initial conditions. We numerically compute estimates for the critical λ, as a function of the material constants, such that the WORS is stable for all λ smaller than this critical value. The critical λ is proportional to the biaxial correlation length, as expected from the numerics in [1]. In Section 6.2, we prove the existence of an OR-type solution on a regular hexagon of edge length λ, where λ is arbitrary, at the fixed temperature. The method of proof is different to that of a square; we appeal to Palais' principle of symmetric criticality [20, 14] and the OR-solution is interpreted differently. We numerically demonstrate that these OR-type solutions are stable on a regular hexagon for λ small enough and the critical stability criterion is again proportional to the biaxial correlation length. This suggests that OR-type solutions may be generic for regular convex polygons with an even number of sides, raising interesting questions about the interplay between geometry, symmetry, temperature and multiplicity of LdG equilibria.

2. Preliminaries. We model nematic profiles on two-dimensional prototype geometries within the LdG theoretical framework. The LdG theory is one of the most powerful continuum theories for nematic liquid crystals and describes the nematic state by a macroscopic order parameter — the LdG $\mathbf{Q}$-tensor that is a macroscopic measure of material anisotropy. The LdG $\mathbf{Q}$-tensor is a symmetric traceless 3×3 matrix i.e. $\mathbf{Q} \in S_0 := \left\{\mathbf{Q} \in \mathbb{M}^{3\times 3} \colon Q_{ij} = Q_{ji},\ Q_{ii} = 0\right\}$. A $\mathbf{Q}$-tensor is said to be (i) isotropic if $\mathbf{Q} = 0$, (ii) uniaxial if $\mathbf{Q}$ has a pair of degenerate non-zero eigenvalues and (iii) biaxial if $\mathbf{Q}$ has three distinct eigenvalues [2, 21]. A uniaxial $\mathbf{Q}$-tensor can be written as $\mathbf{Q}_u = s\left(\mathbf{n} \otimes \mathbf{n} - \mathbf{I}/3\right)$ with $\mathbf{I}$ the 3×3 identity matrix, $s \in \mathbb{R}$ and $\mathbf{n} \in S^2$,

a unit vector. The scalar, s, is an order parameter which measures the degree of orientational order. The vector, $\mathbf{n}$, is referred to as the "director" and labels the single distinguished direction of uniaxial nematic alignment [3, 2].
We work with a simple form of the LdG energy given by

$$I[\mathbf{Q}] := \int_{\Omega} \frac{L}{2} |\nabla \mathbf{Q}|^2 + f_B(\mathbf{Q}) \, \mathrm{dA} \tag{2.1}$$

where $\Omega \subseteq \mathbb{R}^2$ is a two-dimensional domain,

$$|\nabla \mathbf{Q}|^2 := \frac{\partial Q_{ij}}{\partial r_k} \frac{\partial Q_{ij}}{\partial r_k}, \qquad f_B(\mathbf{Q}) := \frac{A}{2} \operatorname{tr} \mathbf{Q}^2 - \frac{B}{3} \operatorname{tr} \mathbf{Q}^3 + \frac{C}{4} \left(\operatorname{tr} \mathbf{Q}^2 \right)^2. \tag{2.2}$$

The variable $A = \alpha(T - T^*)$ is the re-scaled temperature, α, L, B, $C > 0$ are material-dependent constants and T^* is the characteristic nematic supercooling temperature [2, 21]. Further $\mathbf{r} := (x, y)$, $\operatorname{tr} \mathbf{Q}^2 = Q_{ij} Q_{ij}$ and $\operatorname{tr} \mathbf{Q}^3 = Q_{ij} Q_{jk} Q_{ki}$ for i, j, $k = 1, 2, 3$. It is well-known that all stationary points of the thermotropic potential, f_B, are either uniaxial or isotropic [2, 21, 22]. The re-scaled temperature A has three characteristic values: (i) $A = 0$, below which the isotropic phase $\mathbf{Q} = 0$ loses stability, (ii) the nematic-isotropic transition temperature, $A = B^2/27C$, at which f_B is minimized by the isotropic phase and a continuum of uniaxial states with $s = s_+ = B/3C$ and $\mathbf{n}$ arbitrary, and (iii) the nematic superheating temperature, $A = B^2/24C$, above which the isotropic state is the unique critical point of f_B.
We work with $A < 0$ i.e. low temperatures and a large part of the paper focuses on a special temperature, $A = -B^2/3C$, largely because this choice of A facilitates the subsequent analysis. Some of our results can be readily generalized to all temperatures, $A < 0$. For a given $A < 0$, let $\mathscr{N} := \{\mathbf{Q} \in S_0 \colon \mathbf{Q} = s_+ (\mathbf{n} \otimes \mathbf{n} - \mathbf{I}/3)\}$ denote the set of minimizers of the bulk potential, f_B, with

$$s_+ := \frac{B + \sqrt{B^2 + 24|A|C}}{4C}$$

and $\mathbf{n} \in S^2$ arbitrary. In particular, this set is relevant to our choice of Dirichlet conditions for boundary-value problems.
We non-dimensionalize the system using a change of variables, $\bar{\mathbf{r}} = \mathbf{r}/\lambda$, where λ is a characteristic length scale of the system. The re-scaled LdG energy functional is then given by

$$\overline{I}[\mathbf{Q}] := \frac{I[\mathbf{Q}]}{L\lambda} = \int_{\overline{\Omega}} \frac{1}{2} \left| \overline{\nabla} \mathbf{Q} \right|^2 + \frac{\lambda^2}{L} f_B(\mathbf{Q}) \, \overline{\mathrm{dA}}. \tag{2.3}$$

In (2.3), $\overline{\Omega}$ is the re-scaled domain, $\overline{\nabla}$ is the gradient with respect to the re-scaled spatial coordinates and $\overline{\mathrm{d}A}$ is the re-scaled area element. The associated Euler-Lagrange equations are

$$\bar{\Delta} \mathbf{Q} = \frac{\lambda^2}{L} \left\{ A\mathbf{Q} - B \left(\mathbf{Q}\mathbf{Q} - \frac{\mathbf{I}}{3} |\mathbf{Q}|^2 \right) + C |\mathbf{Q}|^2 \mathbf{Q} \right\}, \tag{2.4}$$

where $(\mathbf{Q}\mathbf{Q})_{ik} = Q_{ij} Q_{jk}$ with i, j, $k = 1, 2, 3$. The system (2.4) comprises five coupled nonlinear elliptic partial differential equations. We treat A, B, C, L as fixed constants and vary λ; the analytical results are asymptotic in nature but are validated by numerical simulations for $\lambda \in (0.5 \times 10^{-6}, 0.5 \times 10^{-4})$ m and the LdG theory is believed to be valid for such length scales. In what follows, we drop the *bars* and all statements are to be understood in terms of the re-scaled variables.

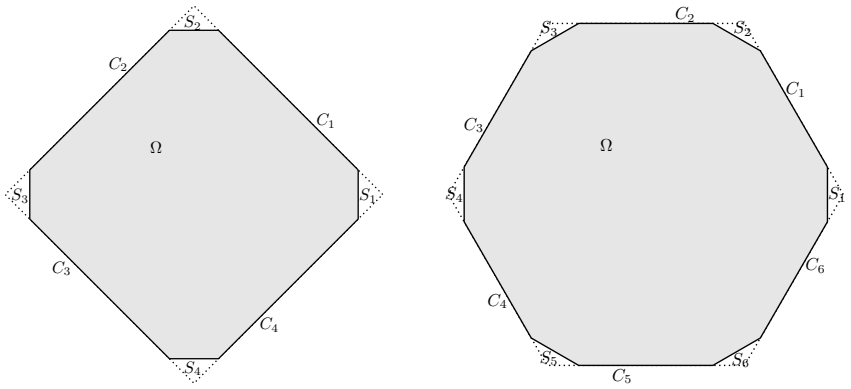

Figure 3.1: Left, the 'truncated square' Ω; right, a 'truncated hexagon' (see Section 6.2). In both cases, a regular polygon is also plotted, in dashed lines.

3. A Scalar Variational Problem for $A = -B^2/3C$. We take $\Omega \subseteq \mathbb{R}^2$ to be a truncated unit square, whose diagonals lie along the axes:

$$\Omega := \left\{(x,\, y) \in \mathbb{R}^2 \colon |x| < 1 - \varepsilon,\ |y| < 1 - \varepsilon,\ |x + y| < 1,\ |x - y| < 1\right\} \tag{3.1}$$

(see Figure 3.1). The boundary, $\partial\Omega$, consists of four "long" edges $C_1, \ldots, C_4$, parallel to the lines $y = x$ and $y = -x$, and four "short" edges $S_1, \ldots, S_4$, of length 2ε, parallel to the x and y-axes respectively. The four long edges C_i are labeled counterclockwise and C_1 is the edge contained in the first quadrant, i.e.

$$C_1 := \left\{(x,\, y) \in \mathbb{R}^2 \colon x + y = 1,\ \varepsilon \le x \le 1 - \varepsilon\right\}.$$

The short edges S_i are introduced to remove the sharp square vertices. They are also labeled counterclockwise and

$$S_1 := \left\{(1 - \varepsilon,\, y) \in \mathbb{R}^2 \colon |y| \le \varepsilon\right\}.$$

We work with Dirichlet conditions on $\partial\Omega$. Following the literature on planar multistable nematic systems [4, 6, 1], we impose *tangent* uniaxial Dirichlet conditions on the long edges, $C_1, \ldots, C_4$. These tangent conditions simply require the uniaxial director to be tangent to the long edges and we fix $\mathbf{Q} = \mathbf{Q}_{\mathrm{b}} \in \mathscr{N}$ on $C_1, \ldots, C_4$ where

$$\mathbf{Q}_{\mathrm{b}}(\mathbf{r}) := \begin{cases} s_+ \left(\mathbf{n}_1 \otimes \mathbf{n}_1 - \dfrac{\mathbf{I}}{3}\right) & \text{for } \mathbf{r} \in C_1 \cup C_3 \\ s_+ \left(\mathbf{n}_2 \otimes \mathbf{n}_2 - \dfrac{\mathbf{I}}{3}\right) & \text{for } \mathbf{r} \in C_2 \cup C_4; \end{cases} \tag{3.2}$$

and

$$\mathbf{n}_1 := \frac{1}{\sqrt{2}}\,(-1,\, 1)\,, \qquad \mathbf{n}_2 := \frac{1}{\sqrt{2}}\,(1,\, 1)\,.$$

We prescribe Dirichlet conditions on the short edges too. The Dirichlet condition on the short edges is defined in terms of a function

$$g(s) := \frac{s_+}{2}\left(e^{-\mu\varepsilon}\frac{e^{\mu s} - e^{-\mu s}}{e^{\mu\varepsilon} - e^{-\mu\varepsilon}} - e^{-\mu s} + 1\right) \quad \text{for } 0 < s < \varepsilon; \qquad \mu := \frac{\lambda B}{(CL)^{1/2}} \tag{3.3}$$

and we take $g(s) = s_+/2$ for $s > \epsilon$ and $g(s) = -g(-s)$ for $s < 0$. We fix $\mathbf{Q} = \mathbf{Q}_\mathrm{b}$ on $S_1, \ldots, S_4$ where

$$\mathbf{Q}_\mathrm{b} := \begin{cases} g(y)\left(\mathbf{n}_1 \otimes \mathbf{n}_1 - \mathbf{n}_2 \otimes \mathbf{n}_2\right) - \dfrac{s_+}{6}\left(2\hat{\mathbf{z}} \otimes \hat{\mathbf{z}} - \mathbf{n}_1 \otimes \mathbf{n}_1 - \mathbf{n}_2 \otimes \mathbf{n}_2\right) & \text{on } S_1 \cup S_3, \\ g(x)\left(\mathbf{n}_1 \otimes \mathbf{n}_1 - \mathbf{n}_2 \otimes \mathbf{n}_2\right) - \dfrac{s_+}{6}\left(2\hat{\mathbf{z}} \otimes \hat{\mathbf{z}} - \mathbf{n}_1 \otimes \mathbf{n}_1 - \mathbf{n}_2 \otimes \mathbf{n}_2\right) & \text{on } S_2 \cup S_4. \end{cases} \tag{3.4}$$

The boundary condition (3.4) is used purely for mathematical convenience in the proofs of Sections 4 and 5. This Dirichlet condition is artificial for two reasons: (i) $\mathbf{Q}_\mathrm{b} \notin \mathscr{N}$ on $S_1, \ldots, S_4$ i.e. $\mathbf{Q}_\mathrm{b}$ is biaxial on these edges and (ii) $\mathbf{Q}_\mathrm{b}$ is not tangent on these edges. However, these edges are short by construction and we conjecture that the qualitative solution trends are not affected by the choice of $\mathbf{Q}_\mathrm{b}$ on $S_1, \ldots, S_4$. Further, we solve the LdG gradient flow model on a square, not a truncated square, in Section 6 and the numerical results are consistent with the analytical results for a truncated square. Given the Dirichlet conditions (3.2) and (3.4), we define our admissible space to be

$$\mathscr{A} := \left\{\mathbf{Q} \in W^{1,2}\left(\Omega,\, S_0\right) \colon \mathbf{Q} = \mathbf{Q}_\mathrm{b} \text{ on } \partial\Omega\right\}. \tag{3.5}$$

It is straightforward to prove the existence of a global minimizer of the re-scaled functional (2.3) in the admissible space $\mathscr{A}$, for all $A < 0$ and for all values of $\lambda > 0$.

We briefly comment on the physical relevance of the boundary conditions in (3.2) and (3.4). In [1], the authors numerically compute LdG equilibria on a three-dimensional (3D) box with six surfaces, impose Dirichlet conditions of the form (3.2) on the lateral surfaces and free boundary conditions on the top and bottom surfaces, which is equivalent to requiring that the profile is independent of the z-coordinate on the top and bottom surfaces. The numerical results in [1] suggest that for such choices of the boundary conditions on a 3D box/well, the profile is indeed translationally invariant and it suffices to study profiles on the bottom cross-section, which is comparable to the truncated square in (3.1). However, free boundary conditions can be difficult to implement in practice. An alternative approach is to impose a surface anchoring energy on the top and bottom surfaces of a 3D box that penalizes any out-of-plane alignment of the nematic molecules and any profile-dependence on the z-coordinate. Indeed in [16], the authors identify a particular form of the surface energy with multiple parameters, such that the surface energy minimizers are of the form (3.6). Informally speaking, they work with thin 3D domains such that the vertical dimension is much smaller than the cross-sectional dimensions and consider the LdG energy on such 3D domains with Dirichlet boundary conditions on the lateral surfaces and surface energies on the top and bottom two-dimensional cross-sections. They prove that the energy minimizers for the 3D problem can be well approximated by appropriately defined energy minimizers on the two-dimensional cross-sections and although we have not made a one-to-one correspondence between their work and our results, the results in [16] suggest that our analysis on a square is applicable to energy minimizers for shallow 3D wells with surface energies on the top and bottom surfaces.

In [1], the authors numerically find the WORS for nano-scale wells or equivalently, for small λ and the WORS $\mathbf{Q}$-tensor solution has two key properties: (i) it has a constant eigenframe, one of which is $\hat{\mathbf{z}}$ and (ii) it is distinguished by an uniaxial cross with negative scalar order parameter (the non-degenerate eigenvalue is negative) along the square diagonals. In the spirit of the numerical results reported in [1], we look for

critical points of (2.3) of the form

$$\begin{aligned}\mathbf{Q}(x,\,y) = q_1(x,\,y)\,(\mathbf{n}_1\otimes\mathbf{n}_1 - \mathbf{n}_2\otimes\mathbf{n}_2) + q_2(x,\,y)\,(\mathbf{n}_1\otimes\mathbf{n}_2 + \mathbf{n}_2\otimes\mathbf{n}_1)\\ + q_3(x,\,y)\,(2\hat{\mathbf{z}}\otimes\hat{\mathbf{z}} - \mathbf{n}_1\otimes\mathbf{n}_1 - \mathbf{n}_2\otimes\mathbf{n}_2)\end{aligned} \tag{3.6}$$

subject to the boundary conditions

$$q_1(x,\,y) = q_{\rm b}(x,\,y) := \begin{cases} s_+/2 & \text{on } C_1\cup C_3\\ -s_+/2 & \text{on } C_2\cup C_4\\ g(y) & \text{on } S_1\cup S_3\\ g(x) & \text{on } S_2\cup S_4;\end{cases} \tag{3.7}$$

$q_2 = 0$ and $q_3 = -s_+/6$ on $\partial\Omega$. Critical points of the form (3.6) mimic the WORS if (i) $q_2 = 0$, and (ii) if $q_1 = 0$ and $q_3 < 0$ on $x = 0$ and $y = 0$ (the square diagonals in our setting), so that $\mathbf{Q} = q_3(x,y)\,(3\hat{\mathbf{z}}\otimes\hat{\mathbf{z}} - \mathbf{I})$ on $x = 0$ and $y = 0$. We first present an existence result for such critical points.

PROPOSITION 3.1. *The LdG Euler-Lagrange equations* (2.4) *admit a solution of the form* (3.6) *on the truncated square,* Ω *defined in* (3.1) *subject to the Dirichlet conditions* (3.2) *and* (3.4)*, provided the functions* q_1*,* q_2*,* q_3 *satisfy the following system*

$$\begin{aligned}\Delta q_1 &= \frac{\lambda^2}{L}\left\{Aq_1 + 2Bq_1q_3 + C\left(2q_1^2 + 2q_2^2 + 6q_3^2\right)q_1\right\}\\ \Delta q_2 &= \frac{\lambda^2}{L}\left\{Aq_2 + 2Bq_2q_3 + C\left(2q_1^2 + 2q_2^2 + 6q_3^2\right)q_2\right\}\\ \Delta q_3 &= \frac{\lambda^2}{L}\left\{Aq_3 + B\left(\frac{1}{3}\left(q_1^2+q_2^2\right) - q_3^2\right) + C\left(2q_1^2 + 2q_2^2 + 6q_3^2\right)q_3\right\}\end{aligned} \tag{3.8}$$

and the boundary conditions in (3.7)*,* $q_2 = 0$ *and* $q_3 = -s_+/6$ *on* $\partial\Omega$ *for arbitrary* $A < 0, B > 0, C > 0, \lambda > 0$ *and* $L > 0$.

Proof. Consider the energy functional $J[q_1,\,q_2,\,q_3]$ defined below:

$$\begin{aligned}J[q_1,q_2,q_3] &:= \int_\Omega \left(|\nabla q_1|^2 + |\nabla q_2|^2 + 3|\nabla q_3|^2\right)\,\mathrm{dA}\\ &+ \int_\Omega \frac{\lambda^2}{L}\left(A\left(q_1^2+q_2^2+3q_3^2\right) + C\left(q_1^2+q_2^2+3q_3^2\right)^2 + 2Bq_3\left(q_1^2+q_2^2\right) - 2Bq_3^3\right)\,\mathrm{dA}.\end{aligned} \tag{3.9}$$

We can prove the existence of a global minimizer of the functional J in (3.9) among the triplets $(q_1,\,q_2,\,q_3) \in W^{1,2}(\Omega,\,\mathbb{R}^3)$ satisfying Dirichlet conditions from the direct methods in the calculus of variations, since J is both coercive and weakly lower semi-continuous [23]. The system of elliptic partial differential equations in (3.8) are simply the Euler-Lagrange equations associated with J in (3.9) and the globally minimizing $(q_1,\,q_2,\,q_3)$ are classical solutions of the system (3.8). Once we obtain the solutions of (3.8), we can construct the corresponding $\mathbf{Q}$-tensor in (3.6) and check that it is an exact solution of the LdG Euler-Lagrange equations in (2.4) by direct substitution. ∎

We do not have results on the multiplicity of solutions of the system (3.8) for arbitrary λ but it is straightforward to check that there is a branch of solutions with $q_2 = 0$ for all $\lambda > 0$ and $A < 0$. This solution branch has a constant eigenframe but we need stronger properties and we henceforth, restrict ourselves to a special temperature

$$A = -\frac{B^2}{3C} \tag{3.10}$$

for which $s_+ = B/C$. This temperature is special because the system (3.8) admits a branch of solutions, $(q_1, q_2, q_3) = (q(x, y), 0, -B/6C)$ at this temperature, consistent with the Dirichlet conditions in (3.7), for all $\lambda > 0$. It is simpler to analyze solutions with just one variable, $q(x, y)$, than solutions with multiple variables and we restrict ourselves to this fixed temperature and solution branch in the rest of this paper.

PROPOSITION 3.2. *For $A = -B^2/3C$ and for all $\lambda > 0$, there exists a branch of solutions of the system* (3.8) *given by*

$$(q_1, 0, q_3) = \left(q_{\min}(x, y), 0, -\frac{B}{6C}\right) \tag{3.11}$$

consistent with the Dirichlet conditions in (3.7)*, $q_2 = 0$ and $q_3 = -\frac{B}{6C}$ on $\partial\Omega$. This branch is defined by a minimizer, $q_{\min}$, of the following energy:*

$$H[q] := \int_\Omega |\nabla q|^2 + \frac{\lambda^2}{L}\left(Cq^4 - \frac{B^2}{2C}q^2\right) \, \mathrm{dA} \tag{3.12}$$

subject to (3.7) *and is hence, a classical solution of*

$$\Delta q = \frac{\lambda^2}{L}\left(2Cq^3 - \frac{B^2}{2C}q\right), \tag{3.13}$$

which is precisely the first equation in (3.8) *with $q_2 = 0$ and $q_3 = -B/6C$. We have the bounds $-\frac{B}{2C} \leq q_{\min} \leq \frac{B}{2C}$.*

Proof. Let $q_{\min}$ be a minimizer of the functional H defined in (3.12), in the admissible space, $X := \{q \in W^{1,2}(\Omega) \colon q \text{ satisfies (3.7) on } \partial\Omega\}$. The existence of a minimizer follows from the direct methods in the calculus of variations. Then $q_{\min}$ is a classical solution of the associated Euler-Lagrange equation (3.13) which ensures that the triplet $(q_1, q_2, q_3) = (q_{\min}, 0, -B/6C)$ is a solution of the system (3.8). This, in turn, yields a critical point of the LdG Euler-Lagrange equations in (2.4) via the representation (3.6). The bounds $-\frac{B}{2C} \leq q_{\min} \leq \frac{B}{2C}$ are a straightforward consequence of the maximum principle and the Dirichlet conditions in (3.7). ∎

LEMMA 3.3. *For any positive B, C and L, there exists $\lambda_0(B, C, L) > 0$ such that, for any $\lambda < \lambda_0(B, C, L)$, the solution branch in Proposition* (3.2) *is the unique critical point of* (2.3) *for $A = -\frac{B^2}{3C}$.*

Proof. This is an immediate consequence of a general uniqueness result for critical points of the energy (2.3) in Lemma 8.2 of [14]. A critical point, $\mathbf{Q}_c$, of the LdG Euler-Lagrange equations in (2.4) is bounded as an immediate consequence of the maximum principle (see [24, 22]) i.e. $|\mathbf{Q}_c| \leq M(A, B, C)$ and the bound M is independent of λ^2/L. The key step is to note that the LdG energy is strictly convex on the set

$$\{\mathbf{Q} \in W^{1,2}(\Omega, S_0) \colon |\mathbf{Q}| \leq M\}$$

for sufficiently small λ i.e. for $\lambda^2/L < \lambda_1(\Omega, A, B, C)$ where the constant λ_1 depends on the domain, temperature and material constants. An explicit computation (for example, by repeating the steps in Lemma 8.2 of [14]) shows that $\lambda_1(\Omega, A, B, C) \approx \frac{C}{16B^2}$ at $A = -\frac{B^2}{3C}$ and we omit the details for brevity. Hence, the LdG energy (2.3) has a unique critical point in this regime.

Let $A = -B^2/3C$; then the triplet $(q_1, q_2, q_3) = (q_{\min}, 0, -B/6C)$ in Proposition 3.2 defines a LdG critical point of the form (3.6) for all $\lambda > 0$. We deduce that this must be the unique LdG critical point for λ small enough from the discussion above. ∎

LEMMA 3.4. *The function $q_{\min} \colon \Omega \to \mathbb{R}$ defined in Proposition 3.2 vanishes along the square diagonals, $x = 0$ and $y = 0$, for $\lambda < \lambda_0$ given by Lemma 3.3.*

Proof. We make the elementary observation that if $q(x, y)$ is a solution of (3.13) subject to (3.7), then so are the functions $q(-x, -y)$, $-q(-x, y)$, $-q(x, -y)$. We combine this symmetry result with the uniqueness result in Lemma 3.3 above to get the desired conclusion for small λ, for example, simply use $q(x, y) = -q(-x, y)$ with $x = 0$ to deduce that $q(0, y) = 0$ and we can use an analogous argument to show that $q = 0$ along $y = 0$. □

From Lemmas 3.3 and 3.4, we deduce that there is a unique LdG critical point

$$\mathbf{Q}_{\min}(x, y) = q_{\min}(x, y)\,(\mathbf{n}_1 \otimes \mathbf{n}_1 - \mathbf{n}_2 \otimes \mathbf{n}_2) - \frac{B}{6C}\,(2\hat{\mathbf{z}} \otimes \hat{\mathbf{z}} - \mathbf{n}_1 \otimes \mathbf{n}_1 - \mathbf{n}_2 \otimes \mathbf{n}_2) \tag{3.14}$$

for sufficiently small λ, where $q_{\min}$ is a global minimizer of H in Proposition 3.2 with $q_{\min} = 0$ on $x = 0$ and $y = 0$. This critical point has a constant eigenframe and has a uniaxial cross of negative scalar order parameter along the square diagonals and hence, has all the qualitative properties of the WORS reported in [1]. However, global minimizers of H need not satisfy the symmetry property, $q_{\min} = 0$ on the coordinate axes, for large λ. This is demonstrated by the following proposition, which characterizes the asymptotic behaviour of $q_{\min}$ as $\lambda \to +\infty$. We introduce the following notation: for any set $E \subseteq \mathbb{R}^2$, we define the Ω-perimeter of E as

$$\mathrm{Per}_\Omega(E) := \sup\left\{\int_E \operatorname{div}\varphi \,\mathrm{dA}\colon \varphi \in C^1_{\mathrm{c}}(\Omega),\ |\varphi| \le 1 \text{ on } \Omega\right\}.$$

If E has a smooth boundary, then the Gauss-Green formula implies that

$$\mathrm{Per}_\Omega(E) = \text{length}\,(\partial E \cap \Omega). \tag{3.15}$$

We denote by $\mathscr{B}$ the class of functions q, defined on Ω, that only take the values $B/2C$, $-B/2C$ and are such that $\mathrm{Per}_\Omega\{q = -B/2C\} < +\infty$. For any $\lambda > 0$, we let $q_{\min,\lambda}$ be a minimizer of H in (3.12).

PROPOSITION 3.5. *There exists a subsequence $\lambda_j \nearrow +\infty$ and a function $q_\infty \in \mathscr{B}$ such that $q_{\min,\lambda_j} \to q_\infty$ in $L^1(\Omega)$ and a.e. Moreover, q_∞ is a minimizer of the functional $J\colon L^1(\Omega) \to (-\infty, +\infty]$ given by*

$$J[q] := k\,\mathrm{Per}_\Omega\left\{q = -\frac{B}{2C}\right\} + \int_{\partial\Omega} \phi(q_{\mathrm{b}}(\mathbf{r}),\, q(\mathbf{r}))\,\mathrm{ds} \tag{3.16}$$

if $q \in \mathscr{B}$, and by $J[q] := +\infty$ otherwise. Here q_{b} is the boundary datum defined by (3.7) *and*

$$\phi(s, t) := 2\sqrt{\frac{C}{L}}\left|\int_s^t \left(\frac{B^2}{4C^2} - \tau^2\right)\mathrm{d}\tau\right| = 2\sqrt{\frac{C}{L}}\left|\frac{1}{3}(s^3 - t^3) - \frac{B^2}{4C^2}(s - t)\right|, \tag{3.17}$$

$$k := \phi\left(-\frac{B}{2C}, \frac{B}{2C}\right) = \frac{B^3}{3C^3}\sqrt{\frac{C}{L}}. \tag{3.18}$$

In Equation (3.16)*, the value $q(\mathbf{r})$ for $\mathbf{r} \in \partial\Omega$ is understood as the inner trace of q at the point $\mathbf{r}$.*

The proof follows on the lines of the analysis in Modica-Mortola [25] and Sternberg [26]. In particular, Proposition 3.5 is a direct consequence of [27, Theorem 7.10], combined with e.g. [27, Theorem 7.3 or 7.11].

We comment on the implications of Proposition 3.5. Suppose that, for any $\lambda > 0$, the minimizer $q_{\min,\lambda}$ mimics the WORS in the sense that $q_{\min,\lambda}(x, y) = 0$ on $x = 0$, $y = 0$. Then, the limit function q_∞ in Proposition 3.5 is

$$q_\infty(x, y) = \begin{cases} B/2C & \text{if } xy > 0 \\ -B/2C & \text{if } xy < 0, \end{cases}$$

with sharp transition layers localized around $x = 0$ or $y = 0$, therefore

$$J[q_\infty] \geq k\mathrm{Per}_\Omega \left\{ q_\infty = -\frac{B}{2C} \right\} = 4k(1 - \varepsilon). \tag{3.19}$$

The last equality follows from (3.15), by noting that the transition layers, i.e. the boundary of the set $\{q_\infty = -B/2C\}$, coincide with the diagonal of the truncated square, whose total length sums up to $4(1 - \varepsilon)$. We consider now the constant function $q = B/2C$, which has no transition layer in the interior of Ω but does not match the Dirichlet boundary condition (3.7). Nevertheless, it is an admissible comparison function for the minimization problem associated with (3.16), for which no boundary condition is imposed. Then, using the symmetry of the problem, the boundary condition (3.7) and (3.17)–(3.18), we have

$$\begin{aligned} J[B/2C] &= \int_{C_2 \cup C_4} \phi \left(-\frac{B}{2C}, \frac{B}{2C} \right) \mathrm{ds} \\ &= k\,\mathrm{Length}\,(C_2 \cup C_4) + 4 \int_{-\varepsilon}^{\varepsilon} \phi \left(g(s), \frac{B}{2C} \right) \mathrm{ds} \\ &\leq 2\sqrt{2}k(1 - \varepsilon) + 8k\varepsilon. \end{aligned} \tag{3.20}$$

In the last inequality, we have used that $|\phi| \leq k$ (which follows from (3.17)–(3.18)) to bound the integral in terms of k. Now, if we take ε sufficiently small, Equations (3.19) and (3.20) imply that $J[q_\infty] > J[B/2C]$, thus contradicting the minimality of q_∞ stated in Proposition 3.5. We conclude that, for large λ, the minimizers, $q_{\min,\lambda}$, of H do not vanish on the coordinate axes. As a consequence, LdG critical points of the form (3.14) mimic the WORS for small λ but not for large λ.
In the next sections, we address the following questions: (i) do we have a WORS-type LdG critical point for all λ and if so, can we provide a semi-analytic description as in (3.14) with a different interpretation of q as a critical point (not a minimizer) of the functional H in Proposition 3.2 and (ii) how does the stability of this critical point depend on the square size measured by λ.

4. The Order Reconstruction Solution. This section is devoted to an analytic definition of the WORS reported in [1] and its qualitative properties. In light of the numerical results in [1], we construct LdG critical points of the form (3.14), such that $q = 0$ on $x = 0$ and $y = 0$. We define the corresponding q's in terms of a critical point, q_{s} of the functional H in Proposition 3.2 and our definition of q_{s} is analogous to saddle solutions of the bistable Allen-Cahn equation studied in [17, 18].
We consider the Euler-Lagrange equations associated with H in Proposition 3.2

$$\begin{cases} -\Delta q + \dfrac{\lambda^2}{L} f(q) = 0 & \text{on } \Omega \\ q = q_{\mathrm{b}} & \text{on } \partial\Omega. \end{cases} \tag{AC}$$

Here, f is given by

$$f(q) := 2Cq^3 - \frac{B^2}{2C}q, \tag{4.1}$$

so the equation (AC) is of the Allen-Cahn type and q_{b} is defined in (3.7).
For a fixed $\lambda > 0$, we define an *OR solution*, or *saddle solution* to be a classical solution $q_{\mathrm{s}} \in C^2(\Omega) \cap C(\overline{\Omega})$ of Problem (AC) that satisfies the sign condition

$$xy\, q_{\mathrm{s}}(x,\, y) \geq 0 \qquad \text{for every } (x,\, y) \in \Omega, \tag{4.2}$$

i.e., q_{s} is non-negative on the first and third quadrant and non-positive elsewhere. In particular, q_{s} vanishes on the coordinate axes. Firstly, we prove the existence and uniqueness of q_{s}, for a fixed $\lambda > 0$.

LEMMA 4.1. *For any $\lambda > 0$, there exists an OR or saddle solution q_{s} for Problem* (AC)*, such that $-B/2C \leq q_{\mathrm{s}} \leq B/2C$.*

Proof. Let Q be the truncated quadrant

$$Q := \Big\{(x,\, y) \in \Omega \colon x > 0,\ y > 0\Big\}. \tag{4.3}$$

We impose boundary conditions

$$q = q_{\mathrm{b}} \quad \text{on } \overline{Q} \cap \partial\Omega, \qquad q = 0 \quad \text{on } \partial Q \setminus \partial\Omega. \tag{4.4}$$

As the boundary datum is continuous and piecewise of class C^1, there exist functions $q \in W^{1,2}(Q)$ that satisfy (4.4). By standard arguments, we find a global minimizer, $q_{\mathrm{s}} \in W^{1,2}(Q)$, of H over Q. We note that $H[q_{\mathrm{s}}] = H[|q_{\mathrm{s}}|]$ and can, hence, assume that $q_{\mathrm{s}} \geq 0$ a.e. on Q.
We define a function on Ω by odd reflection of q_{s} about the coordinate axes. The new function, still denoted by q_{s}, satisfies the sign condition (4.2) and is a weak solution of (AC) on $\Omega \setminus \{0\}$. This function has bounded gradient for fixed λ i.e. $|\nabla q_{\mathrm{s}}| \leq C$ and we can then repeat the arguments in [17, Theorem 3] to deduce that q_{s} is a weak solution of (AC) on Ω (including the origin) for fixed λ. By elliptic regularity on convex polygons (see e.g. [28, Chapter 3]), we have that $q_{\mathrm{s}} \in C^2(\Omega) \cap C(\overline{\Omega})$ is a classical solution of (AC). Finally, the bound $-B/2C \leq q_{\mathrm{s}} \leq B/2C$ is a direct consequence of the maximum principle. ∎

LEMMA 4.2. *For all $\lambda > 0$, there is at most one* non-negative *solution $q \in C^2(Q) \cap C(\overline{Q})$ to the problem*

$$\begin{cases} -\Delta q + \dfrac{\lambda^2}{L} f(q) = 0 & \text{on } Q \\ q = q_{\mathrm{b}} & \text{on } \overline{Q} \cap \partial\Omega \\ q = 0 & \text{on } \partial Q \setminus \partial\Omega. \end{cases} \tag{AC$'$}$$

There is a unique non-negative OR solution, $q_{\mathrm{s}} : \Omega \to \mathbb{R}$, defined in terms of q above.

Proof. Our proof is analogous to [17, Lemma 1]. Consider two non-negative solutions q_1, q_2 to (AC$'$). Then $q := \max\{q_1,\, q_2\}$ is a subsolution to Problem (AC$'$) (see e.g. [29]), i.e. $q \in W^{1,2}(Q)$ and

$$\int_Q \left(\nabla q \cdot \nabla\varphi + \frac{\lambda^2}{L} f(q)\varphi\right) \mathrm{dA} \leq 0 \qquad \text{for any } \varphi \in W_0^{1,2}(Q) \text{ s.t. } \varphi \geq 0$$

$$q \leq q_{\mathrm{b}} \qquad \text{on } \partial Q \cap \partial\Omega, \qquad q \leq 0 \qquad \text{on } \partial Q \setminus \partial\Omega.$$

The maximum principle, applied to both q_1 and q_2, implies that $q \le B/2C$, so the constant $B/2C$ is a supersolution to (AC′). Therefore, by the classical sub- and supersolution method (see, e.g., [23, Theorem 1 p. 508]), there exists a solution p_2 of (AC′) such that $q \le p_2 \le B/2C$, so that

$$0 \le q_1 \le p_2 \qquad \text{on } Q. \tag{4.5}$$

We multiply the equation for p_2 with q_1, multiply the equation for q_1 with p_2, integrate by parts and take the difference to obtain

$$\frac{\lambda^2}{L}\int_Q \Big(f(p_2)q_1 - f(q_1)p_2\Big)\,\mathrm{dA} = \int_{\partial Q}\left(\frac{\partial p_2}{\partial \mathbf{n}}q_1 - \frac{\partial q_1}{\partial \mathbf{n}}p_2\right)\mathrm{ds},$$

where $\mathbf{n}$ is the outward normal to ∂Q. Recalling the definition (4.1) of f and the boundary conditions (4.4), we have

$$\frac{2C\lambda^2}{L}\int_Q q_1 p_2\left(p_2^2 - q_1^2\right)\,\mathrm{dA} = \int_{\overline{Q}\cap\partial\Omega} q_{\mathrm{b}}\left(\frac{\partial p_2}{\partial \mathbf{n}} - \frac{\partial q_1}{\partial \mathbf{n}}\right)\mathrm{ds}.$$

The left-hand side is non-negative, because of (4.5), while the right-hand side is non-positive (due to (4.5) and $p_2 = q_1$ on ∂Q); therefore, both sides of the equality must vanish. The strong maximum principle [29, Theorem 3.5] states that, if a non-negative solution q of Equation (AC) satisfies $q(\mathbf{r}_0) = 0$ at some internal point $\mathbf{r}_0 \in \Omega$, then in fact $q = 0$ everywhere. Since $q_1 \not\equiv 0$, we deduce that $q_1 > 0$ in the interior of Q, which yields $p_2 > 0$ in Q, thanks to (4.5). Thus, we deduce

$$q_1 = p_2 \ge \max\{q_1,\, q_2\} \qquad \text{on } Q$$

and, in particular, $q_1 \ge q_2$ on Q. By a symmetric argument, we obtain $q_1 \le q_2$ on Q and the conclusion follows.

We can repeat the arguments of Lemma 4.2 on the remaining three quadrants to deduce that the OR solution is unique on Ω. □

The choice of the Dirichlet condition on the short edges (see (3.7)) in terms of the function g defined in (3.3) is motivated by the fact that g satisfies the inequality

$$-Lg'' + \frac{\lambda^2 B^2}{C}g - \frac{\lambda^2 B^3}{2C^2} = 0, \quad g' \ge 0 \quad \text{and} \quad 0 < g < \frac{B}{2C} \qquad \text{on } (0,\, \varepsilon), \tag{4.6}$$

and hence,

$$-\lambda^2 f(g) = \frac{\lambda^2 B^2}{2C}g\left(1 + \frac{2C}{B}g\right)\left(1 - \frac{2C}{B}g\right) \le \frac{\lambda^2 B^3}{2C^2}\left(1 - \frac{2C}{B}g\right) = -Lg''. \tag{4.7}$$

We can hence, use g to construct supersolutions for the Problem (AC′).

LEMMA 4.3. *For any $\lambda > 0$, we have*

$$\frac{\partial q_{\mathrm{s}}}{\partial \mathbf{n}} \ge 0 \qquad \text{on } \{(x,\, y) \in \partial\Omega\colon x > 0,\ y > 0\},$$

where $\mathbf{n}$ is the outward-pointing normal to Ω. In fact, we have the strict inequality

$$\frac{\partial q_{\mathrm{s}}}{\partial \mathbf{n}} > 0 \qquad \text{on } \Gamma := \{(x,\, y) \in \partial\Omega\colon x > \varepsilon,\ y > \varepsilon\}. \tag{4.8}$$

Proof. We consider the function $p\colon \overline{Q} \to \mathbb{R}$ defined by

$$p(x,y) := \begin{cases} g(y) & \text{if } 0 \le y < \varepsilon \\ B/2C & \text{if } \varepsilon \le y \le 1-\varepsilon. \end{cases}$$

It is straightforward to check that p is a weak supersolution for Problem (AC′), from (4.6). Moreover, $p \ge 0$ and the constant, 0, is a subsolution for Problem (AC′). The standard sub- and supersolution method, combined with the uniqueness result in Lemma 4.2, implies that $q_{\mathrm{s}} \le p$ on Q. Moreover, $q_{\mathrm{s}} = p$ on

$$\Gamma_x := \{(x,\, y) \in \partial\Omega\colon x > \varepsilon,\ y > 0\}\,,$$

and hence,

$$\frac{\partial q_{\mathrm{s}}}{\partial \mathbf{n}} \ge \frac{\partial p}{\partial \mathbf{n}} \qquad \text{on } \Gamma_x.$$

(Indeed, should the opposite inequality $\partial q_{\mathrm{s}}/\partial\mathbf{n}(\mathbf{r}_0) < \partial p/\partial\mathbf{n}(\mathbf{r}_0)$ be true at some point $\mathbf{r}_0 \in \Gamma_x$, by Taylor-expanding the function $q_{\mathrm{s}} - p$ at the point $\mathbf{r}_0$ in the direction $-\mathbf{n}$ we would find that $q_{\mathrm{s}} > p$ locally near $\mathbf{r}_0$, which contradicts $q_{\mathrm{s}} \le p$.) Since $\partial p/\partial\mathbf{n} = 0$ on Γ_x, we conclude that $\partial q_{\mathrm{s}}/\partial\mathbf{n} \ge 0$ on Γ_x. A symmetric argument yields

$$\frac{\partial q_{\mathrm{s}}}{\partial \mathbf{n}} \ge 0 \qquad \text{on } \Gamma_y := \{(x,\, y) \in \partial\Omega\colon x > 0,\ y > \varepsilon\}\,.$$

Finally, we notice that $w := B/2C - q_{\mathrm{s}}$ satisfies $0 \le w \le B/2C$,

$$-\Delta w + \frac{2C\lambda^2}{L} w \underbrace{\left(\frac{B}{2C} - w\right)\left(\frac{B}{C} - w\right)}_{\ge 0} = 0 \qquad \text{on } Q,$$

and w attains its minimum value $w = 0$ at each point of Γ. Then, the Hopf lemma (see e.g. [29, Lemma 3.4 p. 34]) yields $\partial w/\partial\mathbf{n} < 0$ on Γ, whence (4.8) follows.
□

Now, we use Lemma 4.3 to show that q_{s} can be extended to a weak supersolution p_{s} to the Allen-Cahn equation (AC), defined on the infinite open quadrant $K := (0,\, +\infty)^2$. We divide the quadrant K into four parts: $K_0 := Q$, K_1 and K_2 are two semi-infinite strips

$$K_1 := [1-\varepsilon,\, +\infty) \times [0,\, \varepsilon], \qquad K_2 := [0,\, \varepsilon] \times [1-\varepsilon,\, +\infty)$$

and $K_3 := K \setminus (K_0 \cup K_1 \cup K_2)$ and we define $p_{\mathrm{s}}\colon K \to \mathbb{R}$ by

$$p_{\mathrm{s}}(x,\, y) := \begin{cases} q_{\mathrm{s}}(x,\, y) & \text{on } K_0 = Q \\ g(y) & \text{on } K_1 \\ g(x) & \text{on } K_2 \\ B/2C & \text{on } K_3. \end{cases} \tag{4.9}$$

Lemma 4.4. *The function $p_{\mathrm{s}} \in W^{1,2}_{\mathrm{loc}}(K)$ is a weak supersolution of the Allen-Cahn equation, that is, for every non-negative function $\varphi \in C^1_{\mathrm{c}}(K)$, we have*

$$\int_K \left\{ \nabla p_{\mathrm{s}} \cdot \nabla\varphi + \frac{\lambda^2}{L} f(p_{\mathrm{s}})\varphi \right\} \mathrm{dA} \ge 0.$$

This lemma follows directly from Lemma 4.3 and the assumptions (4.6)–(4.7) on the boundary datum g. The details of the proof are omitted, for the sake of brevity.
We conclude this section by studying the first derivatives of q_s on the quadrant Q; by symmetry, this gives us information about the derivatives of q_s on Ω.

LEMMA 4.5. *For any $\lambda > 0$, the OR solution is monotonically increasing in the x and y directions, on the quadrant Q:*

$$\frac{\partial q_s}{\partial x} > 0, \quad \frac{\partial q_s}{\partial y} > 0 \qquad \text{on } Q.$$

Proof. This argument is inspired by [17, Theorem 2]. We first claim that q_s is non-decreasing in the x-direction, that is,

$$q_s(x, y) \leq q_s(x + \tau, y) \qquad \text{for any } \tau > 0,\ (x, y) \in Q \text{ s.t. } (x + \tau, y) \in Q. \tag{4.10}$$

Let Q_τ be the translated domain $Q_\tau := Q + (\tau, 0)$. We consider Problem (AC'_τ), i.e. the analogue of Problem (AC') on the translated domain Q_τ. By translation invariance, the unique non-negative solution to Problem (AC'_τ) is given by

$$q_\tau(x + \tau, y) := q_s(x, y) \qquad \text{for any } (x, y) \in Q. \tag{4.11}$$

Moreover, from Lemma 4.4, the function p_s in (4.9) is a non-negative supersolution of (AC'_τ). The sub- and supersolution method combined with the uniqueness of solutions for Problem (AC'_τ) (Lemma 4.2) implies that

$$q_\tau(x + \tau, y) \leq p_s(x + \tau, y) \qquad \text{for any } (x, y) \in Q \text{ s.t. } (x + \tau, y) \in Q.$$

Recalling (4.11) and using that $p_s = q_s$ on Q, we conclude the proof of (4.10).
Next, let us set $u := \partial q_s / \partial x$. By (4.10), we know that $u \geq 0$ on Q; we want to prove that the strict inequality holds. We differentiate Equation (AC') with respect to x:

$$\Delta u - \frac{\lambda^2}{L} f'(q_s) u = 0 \qquad \text{on } Q.$$

By the strong maximum principle [29, Theorem 3.5] we deduce that either $u \equiv 0$ in Q (that is, q_s only depends of y) or $u > 0$ in Q. The first possibility is clearly inconsistent with the boundary conditions, therefore u must be strictly positive inside Q. A similar argument can be applied to the derivative with respect to y. ∎
We combine the results from Sections 3 and 4 to state the following.

LEMMA 4.6. *We define an OR LdG critical point of the energy* (2.3) *on Ω, at a fixed temperature $A = -B^2/3C$, subject to the Dirichlet conditions* (3.2) *and* (3.4) *to be*

$$\mathbf{Q}_s(x, y) := q_s(x, y)\,(\mathbf{n}_1 \otimes \mathbf{n}_1 - \mathbf{n}_2 \otimes \mathbf{n}_2) - \frac{B}{6C}\,(2\hat{\mathbf{z}} \otimes \hat{\mathbf{z}} - \mathbf{n}_1 \otimes \mathbf{n}_1 - \mathbf{n}_2 \otimes \mathbf{n}_2) \tag{4.12}$$

where q_s is the OR or saddle solution of Problem (AC')*, defined in Lemma 4.1. The critical point, $\mathbf{Q}_s$, exists for all λ and all L and is the unique LdG critical point, and hence globally stable, for sufficiently small λ.*

Comment on proof. Lemma 4.6 is immediate from Proposition 3.1, 3.2 and Lemma 4.1. The uniqueness follows from Lemmas 4.1 and 3.3. ∎

5. Instability of the OR LdG critical point. We study the stability of $\mathbf{Q}_{\mathrm{s}}$ in terms of the stability of q_{s} as a critical point of the functional H defined in Proposition 3.2. In this section, when we need to stress the dependence λ, we write $q_{\mathrm{s},\lambda}$ and H_λ instead of q_{s}, H. The final aim of this section is to prove

THEOREM 5.1. *For any positive parameters B, C and L, there exists a unique value $\lambda_{\mathrm{c}} > 0$ such that a pitchfork bifurcation arises at $(\lambda_{\mathrm{c}}, q_{\mathrm{s},\lambda_{\mathrm{c}}})$. More precisely, there exist positive numbers ϵ, δ and two smooth maps*

$$t \in (-\delta,\, \delta) \mapsto \lambda(t) \in (\lambda_{\mathrm{c}} - \epsilon,\, \lambda_{\mathrm{c}} + \epsilon), \qquad t \in (-\delta,\, \delta) \mapsto h_t \in W^{1,2}_0(\Omega)$$

such that all the pairs $(\lambda,\, q) \in \mathbb{R}^+ \times W^{1,2}(\Omega)$ satisfying

$$q \text{ is a solution to (AC)}, \qquad |\lambda - \lambda_{\mathrm{c}}| \leq \epsilon, \qquad \|q - q_{\mathrm{s},\lambda_{\mathrm{c}}}\|_{W^{1,2}(\Omega)} \leq \epsilon$$

are either

$$(\lambda,\, q) = (\lambda,\, q_{\mathrm{s},\lambda}) \qquad \text{or} \qquad \begin{cases} \lambda = \lambda(t) \\ q = q_{\mathrm{s},\lambda(t)} + t\eta_{\lambda_{\mathrm{c}}} + t^2 h_t. \end{cases}$$

Here $\eta_{\lambda_{\mathrm{c}}} \in W^{1,2}_0(\Omega)$ is an eigenfunction corresponding to the loss of stability at λ_{c}, that is, $\eta_{\lambda_{\mathrm{c}}} \not\equiv 0$ is a solution of

$$\Delta \eta_{\lambda_{\mathrm{c}}} = \frac{\lambda_{\mathrm{c}}^2}{L}\left(6C q_{\mathrm{s},\lambda_{\mathrm{c}}}^2 - \frac{B^2}{2C}\right)\eta_{\lambda_{\mathrm{c}}} \qquad \text{on } \Omega. \tag{5.1}$$

Therefore, for fixed $B, C, L > 0$, $q_{s,\lambda}$ exists as a critical point of the functional, H, defined in Proposition 3.2 for all $\lambda > 0$ and loses stability for $\lambda > \lambda_{\mathrm{c}}$.

Equation (5.1) can be derived formally by plugging the ansatz $q = q_{\mathrm{s},\lambda(t)} + t\eta_{\lambda_{\mathrm{c}}} + \mathrm{O}(t^2)$ into (AC) and retaining only linear terms in t. More rigorously, (5.1) is the Euler-Lagrange equation for the second variation of the energy, see (5.3) below. The proof of Theorem 5.1 follows the same paradigm as [14, Theorem 5.2] and we address the necessary technical differences since the author studies a one-dimensional order reconstruction problem in [14] and we have a two-dimensional problem at hand.

We introduce some notation for functional spaces. We denote by

$$X := \left\{q \in W^{1,2}(\Omega) \colon q = q_{\mathrm{b}} \text{ on } \partial\Omega\right\}$$

the space of admissible functions.We also define the spaces Y, Y_0 as follows:

$$Y := \left\{q \in X \colon xy\, q(x,\, y) \geq 0 \text{ for a.e. } (x,\, y) \in \Omega\right\}.$$

The space Y_0 is defined in a similar way, except that the condition $q \in X$ is replaced by $q \in W^{1,2}_0(\Omega)$. Every function in Y or Y_0 vanishes along the axes, in the sense of traces. The space Y is a closed affine subspace of X, whose direction is Y_0. We always endow X, Y, Y_0 with the topology induced by the $W^{1,2}$-norm.

Lemma 4.2 implies that $q_{\mathrm{s},\lambda}$ is the only non-negative solution of (AC) that belongs to Y. The stability of $q_{\mathrm{s},\lambda}$ is measured by the quantity

$$\mu(\lambda) := \inf_{\eta \in W^{1,2}_0(\Omega)\setminus\{0\}} \frac{\delta^2 H_\lambda[\eta]}{\int_\Omega \eta^2}, \tag{5.2}$$

where $\delta^2 H_\lambda$ is the second variation of H_λ at $q_{\mathrm{s},\lambda}$, given by

$$\delta^2 H_\lambda[\eta] := \frac{\mathrm{d}^2}{\mathrm{d}t^2}_{|t=0} H_\lambda[q_{\mathrm{s},\lambda} + t\eta] = \int_\Omega \left\{|\nabla \eta|^2 + \frac{\lambda^2}{L}\left(6C q_{\mathrm{s},\lambda}^2 - \frac{B^2}{2C}\right)\eta^2\right\} \mathrm{dA}. \tag{5.3}$$

In other words, $\mu(\lambda)$ is the first eigenvalue of $\delta^2 H_\lambda$. By classical arguments (e.g., by adapting the arguments in [29, Theorem 8.38]), one sees that $\mu(\lambda)$ is a simple eigenvalue, and every eigenfunction $\eta \not\equiv 0$ associated with $\mu(\lambda)$ is either strictly positive everywhere in Ω or strictly negative everywhere in Ω.

LEMMA 5.2. *The map $(0, +\infty) \to Y$ defined by $\lambda \mapsto q_{\mathrm{s},\lambda}$ is smooth.*

Proof. We claim that, for any $\lambda > 0$, there exists a positive constant $\alpha(\lambda)$ such that

$$\delta^2 H_\lambda[\eta] \geq \alpha(\lambda) \int_\Omega |\nabla \eta|^2 \, \mathrm{dA} \qquad \text{for any } \eta \in Y_0. \tag{5.4}$$

Once we prove the inequality (5.4), we can apply the implicit function theorem as in [14, proof of Proposition 4.3] to obtain that $\lambda \mapsto q_{\mathrm{s},\lambda}$ is smooth. We prove (5.4) with the help of an Hardy-type trick. Fix $\lambda > 0$ and a test function $\eta \in Y_0$. (Now λ is fixed, so we omit in the notation for q_s and H.) The function η vanishes along the square diagonals or the coordinate axes. By an approximation argument, we can assume WLOG that η is smooth and its support does not intersect the square diagonals. In particular, we have $q_\mathrm{s}(x, y) \neq 0$ for any $(x, y) \in \mathrm{support}(\eta)$. Therefore, there exists a smooth function $v \colon \overline{\Omega} \to \mathbb{R}$ such that $\eta = q_\mathrm{s} v$. Substituting $\eta = q_\mathrm{s} v$ into (5.3) and using (AC), we obtain

$$\delta^2 H[\eta] = \int_\Omega \left\{ \left(|\nabla q_\mathrm{s}|^2 v^2 + 2 q_\mathrm{s} v \nabla q_\mathrm{s} \cdot \nabla v + |\nabla v|^2 q_\mathrm{s}^2 \right) + \left(\Delta q_\mathrm{s} + 4 \frac{\lambda^2}{L} C q_\mathrm{s}^3 \right) q_\mathrm{s} v^2 \right\} \mathrm{dA}.$$

An integration by parts yields $\int_\Omega q_\mathrm{s} v^2 \Delta q_\mathrm{s} \, \mathrm{dA} = -\int_\Omega \left\{ |\nabla q_\mathrm{s}|^2 v^2 + 2 q_\mathrm{s} v \nabla q_\mathrm{s} \cdot \nabla v \right\} \mathrm{dA}$. All the boundary terms vanish because $v = \eta = 0$ on $\partial\Omega$. Therefore, we have

$$\delta^2 H[\eta] = \int_\Omega \left\{ |\nabla v|^2 + \frac{4\lambda^2 C}{L} q_\mathrm{s}^2 v^2 \right\} q_\mathrm{s}^2 \, \mathrm{dA} \geq 0$$

for any $\eta \in Y_0$, with equality if and only if $\eta = 0$. The inequality (5.4) now follows from a standard argument (e.g., one can argue by contradiction and use the compact embedding of Y_0 into $L^2(\Omega)$). ∎

We now consider the re-scaled functions $\tilde{q}_{\mathrm{s},\lambda} \colon \lambda\Omega \to \mathbb{R}$ defined by $\tilde{q}_{\mathrm{s},\lambda}(x, y) := q_{\mathrm{s},\lambda}\left(\frac{x}{\lambda}, \frac{y}{\lambda}\right)$ for $(x, y) \in \lambda\Omega$, which satisfy the equation

$$-\Delta \tilde{q}_{\mathrm{s},\lambda} + \frac{1}{L} f(\tilde{q}_{\mathrm{s},\lambda}) = 0 \qquad \text{on } \lambda\Omega, \tag{5.5}$$

with appropriate boundary conditions for $\tilde{q}_{\mathrm{s},\lambda}$.

LEMMA 5.3. *For any $\lambda > 0$ and any $(x, y) \in \lambda Q = \{\lambda\Omega \cap \{x, y \geq 0\}\}$, we have*

$$\frac{\partial \tilde{q}_{\mathrm{s},\lambda}}{\partial \lambda}(x, y) < 0.$$

Proof. We first show that $\tilde{q}_{\mathrm{s},\lambda}$ is non-increasing as a function of λ. We take $\lambda_1 < \lambda_2$ and, for simplicity, we set $\tilde{q}_j := \tilde{q}_{\mathrm{s},\lambda_j}$ for $j \in \{1, 2\}$. We claim that

$$\tilde{q}_1(x, y) \geq \tilde{q}_2(x, y) \qquad \text{for any } (x, y) \in \lambda_1\Omega. \tag{5.6}$$

We extend $\tilde{q}_1$ to a new function $\tilde{p}_1$, defined over the infinite quadrant $K = (0, +\infty)^2$, so that $\tilde{p}_1$ is a weak supersolution of (5.5) on K. We define $\tilde{p}_1$ as in Equation (4.9),

with the obvious modifications due to the scaling $\Omega \to \lambda\Omega$. Then the function $\tilde{p}_1$ satisfies

$$\begin{cases} \displaystyle\int_{\lambda_2\Omega} \left(\nabla\tilde{p}_1 \cdot \nabla\varphi + \frac{1}{L} f(\tilde{p}_1)\varphi \right) \mathrm{dA} \geq 0 & \text{for any } \varphi \in W_0^{1,2}(\lambda_2 Q),\ \varphi \geq 0 \\ \tilde{p}_1 \geq \tilde{q}_2 & \text{on } \partial(\lambda_2 Q). \end{cases}$$

The sub- and supersolution method, combined with the uniqueness result in Lemma 4.2 and a scaling argument, imply that $\tilde{p}_1 \geq \tilde{q}_2$ on $\lambda_2\Omega$. Since $\tilde{p}_1 = \tilde{q}_1$ on $\lambda_1\Omega$, we conclude that (5.6) holds.
Now, fix $\lambda > 0$. It follows from (5.6) that $v := \partial\tilde{q}_{\mathrm{s},\lambda}/\partial\lambda \leq 0$ on $\lambda\Omega$. We differentiate Equation (5.5) with respect to λ and show that v satisfies

$$-\Delta v + \frac{1}{L} f'(\tilde{q}_{\mathrm{s},\lambda}) v = 0 \qquad \text{on } \lambda\Omega.$$

By the strong maximum principle [29, Theorem 3.5], we conclude that either $v \equiv 0$ on $\lambda\Omega$ or $v < 0$ on $\lambda\Omega$. However, $\tilde{q}_{\mathrm{s},\lambda}$ satisfies the boundary condition

$$\tilde{q}_{\mathrm{s},\lambda}\left(\frac{\lambda}{2}, \frac{\lambda}{2}\right) = q_{\mathrm{s},\lambda}\left(\frac{1}{2}, \frac{1}{2}\right) = \frac{B}{2C}.$$

Differentiating with respect to λ, we obtain

$$v\left(\frac{\lambda}{2}, \frac{\lambda}{2}\right) + \frac{1}{2\sqrt{2}} \frac{\partial\tilde{q}_{\mathrm{s},\lambda}}{\partial\mathbf{n}}\left(\frac{\lambda}{2}, \frac{\lambda}{2}\right) = 0,$$

where $\mathbf{n}$ is the outward-pointing normal to $\partial\Omega$. Since the normal derivative is strictly positive (by Lemma 4.3 and a scaling argument), we conclude that $v(\lambda/2, \lambda/2) < 0$. Therefore, v cannot vanish identically and, by the strong maximum principle, it must be strictly negative everywhere on $\lambda\Omega$. ∎

LEMMA 5.4. *The map $(0, +\infty) \to \mathbb{R}$ defined by $\lambda \mapsto \mu(\lambda)$ is smooth and $\mu'(\lambda) < 0$ for any $\lambda > 0$.*

Proof. The smoothness of μ can be proven as in [14, Proposition 4.3]. We now prove that $\mu'(\lambda) < 0$ for any $\lambda > 0$. By Equation (5.2) and a scaling argument, for any $\lambda > 0$, we have

$$\mu(\lambda) = \inf_{\eta} \int_{\lambda\Omega} \left\{ |\nabla\eta|^2 + \frac{1}{L}\left(6C\tilde{q}_{\mathrm{s},\lambda}^2 - \frac{B^2}{2C}\right)\eta^2 \right\} \mathrm{dA}. \tag{5.7}$$

The infimum is taken over all $\eta \in W_0^{1,2}(\lambda\Omega)$ such that $\int_{\lambda\Omega} \eta^2 = 1$. Fix $\lambda_0 > 0$ and let $\eta_0 \in W_0^{1,2}(\lambda_0\Omega)$ be a minimizer for (5.7). We extend η_0 to be zero outside $\lambda_0\Omega$. Then, for any $\lambda \geq \lambda_0$, we have

$$\mu(\lambda) \leq \mu_0(\lambda) := \int_{\lambda_0\Omega} \left\{ |\nabla\eta_0|^2 + \frac{1}{L}\left(6C\tilde{q}_{\mathrm{s},\lambda}^2 - \frac{B^2}{2C}\right)\eta_0^2 \right\} \mathrm{dA},$$

with equality if $\lambda = \lambda_0$. This implies

$$\mu'(\lambda_0) \leq \mu_0'(\lambda_0) = \frac{12C}{L} \int_{\lambda_0\Omega} \tilde{q}_{\lambda_0,\mathrm{s}} \frac{\mathrm{d}\tilde{q}_{\mathrm{s},\lambda}}{\mathrm{d}\lambda}_{|\lambda=\lambda_0} \eta_0^2 \,\mathrm{dA}.$$

By Lemma 5.3 and the odd symmetry of $q_{s,\lambda}$ about the axes, the integrand is non-positive and it does not vanish identically. Therefore, the right-hand side is strictly negative and so is $\mu'(\lambda_0)$. □

LEMMA 5.5. *There exists a positive number λ^* such that $\mu(\lambda) < 0$ for any $\lambda \geq \lambda^*$.*

Proof. The uniform bound $|q_{s,\lambda}| \leq B/2C$ and [30, Lemma A.2], applied to the Equation (AC), yield the estimate $|\nabla q_{s,\lambda}| \leq C\lambda$ for some λ-independent constant C. By scaling, we obtain $|\tilde{q}_{s,\lambda}| + |\nabla \tilde{q}_{s,\lambda}| \leq C$. Therefore, by the Ascoli-Arzelà theorem, we have the locally uniform convergence $\tilde{q}_{s,\lambda} \to \tilde{q}_\infty$ as $\lambda \to +\infty$, up to a non-relabelled subsequence. Taking the limit in both sides of (5.5), we see that $\tilde{q}_\infty$ is the unique saddle solution of the Allen-Cahn equation (5.5) on $\mathbb{R}^2$ (see [17]). Thanks to [18, Lemma 3.4], we find a function $\eta \in H^2(\mathbb{R}^2)$ such that

$$\int_{\mathsf{R}^2} \left\{ |\nabla \eta|^2 + \frac{1}{L} \left(6C\tilde{q}_\infty^2 - \frac{B^2}{2C} \right) \eta^2 \right\} \, \mathrm{dA} < 0.$$

By truncation, we can assume WLOG that η has compact support. Then, using the locally uniform convergence $\tilde{q}_{s,\lambda} \to \tilde{q}_\infty$, we conclude that the right-hand side of (5.7) becomes negative for λ large enough, whence $\mu(\lambda) < 0$ for λ large enough. □

We revert to the original re-scaled domain, Ω, and to the original function, $q_{s,\lambda}$, for the rest of the computation.

Proof of Theorem 5.1 We know that $\mu(\lambda) > 0$ for $0 < \lambda \ll 1$: this follows from the stability result for the full LdG system in Lemma 3.3. (This can also be proved directly from (5.7), by applying Poincaré inequality.) From Lemma 5.5, we can find $\lambda_c > 0$ such that $\mu(\lambda_c) = 0$. Such a λ_c is unique, because μ is strictly decreasing (Lemma 5.4). To show that a pitchfork bifurcation arises at $\lambda = \lambda_c$, we apply the Crandall and Rabinowitz bifurcation theorem [31, Theorem 1.7] to the operator $\mathscr{F}$ defined by

$$\mathscr{F}(\lambda, h) := -\Delta(q_{s,\lambda} + h) + \frac{\lambda^2}{L} f(q_{s,\lambda} + h)$$

for any $(\lambda, h) \in \mathbb{R}^+ \times W_0^{1,2}(\Omega)$. We first have to check that the assumptions of the theorem are satisfied. Clearly, we have $\mathscr{F}(\lambda, 0) = 0$ for any $\lambda > 0$. The map $\mathscr{F}$ is smooth and we have

$$\mathrm{D}_h \mathscr{F}(\lambda, 0) = -\Delta + \frac{\lambda^2}{L} f'(q_{s,\lambda}).$$

This is a Fredholm operator of index 0, whose smallest eigenvalue $\mu(\lambda)$ has multiplicity 1. Therefore, for $\lambda = \lambda_c$, we have

$$\dim \frac{H^{-1}(\Omega)}{\mathrm{range}\, \mathrm{D}_h \mathscr{F}(\lambda_c, 0)} = \dim \mathrm{kernel}\, \mathrm{D}_h \mathscr{F}(\lambda_c, 0) = 1.$$

Let η_λ be an eigenfunction associated with $\mu(\lambda)$ (i.e., a minimiser for (5.2)), renormalised so that $\int_\Omega \eta_\lambda^2 = 1$. From [32, Lemma 1.3], we can assume that the map $\lambda \mapsto \eta_\lambda$ is smooth, at least for λ close enough to λ_c. In order to apply Crandall and Rabinowitz's theorem, we need to check that

$$\mathrm{D}_\lambda \mathrm{D}_h \mathscr{F}(\lambda_c, 0)[\eta_{\lambda_c}] \notin \mathrm{range}\, \mathrm{D}_h \mathscr{F}(\lambda_c, 0).$$

Proceeding by contradiction, assume that there exists $h \in W_0^{1,2}(\Omega)$ such that

$$\mathrm{D}_\lambda \mathrm{D}_h \mathscr{F}(\lambda_c, 0)[\eta_{\lambda_c}] = \mathrm{D}_h \mathscr{F}(\lambda_c, 0)[h]. \tag{5.8}$$

Then, using the fact that $\mathrm{D}_h\mathscr{F}(\lambda, 0)$ is symmetric and $\eta_{\lambda_\mathrm{c}} \in \ker \mathrm{D}_h\mathscr{F}(\lambda_\mathrm{c}, 0)$, we obtain that

$$\begin{aligned}\mu'(\lambda_\mathrm{c}) &= \frac{\mathrm{d}}{\mathrm{d}\lambda}_{|\lambda=\lambda_\mathrm{c}} \langle \mathrm{D}_h\mathscr{F}(\lambda, 0)[\eta_\lambda], \eta_\lambda\rangle \\ &= \langle \mathrm{D}_\lambda\mathrm{D}_h\mathscr{F}(\lambda_\mathrm{c}, 0)[\eta_{\lambda_\mathrm{c}}], \eta_{\lambda_\mathrm{c}}\rangle + 2\langle \mathrm{D}_h\mathscr{F}(\lambda_\mathrm{c}, 0)[\eta_{\lambda_\mathrm{c}}], \partial_\lambda\eta_{\lambda|\lambda=\lambda_\mathrm{c}}\rangle \\ &= \langle \mathrm{D}_h\mathscr{F}(\lambda_\mathrm{c}, 0)[h], \eta_{\lambda_\mathrm{c}}\rangle \\ &= \langle \mathrm{D}_h\mathscr{F}(\lambda_\mathrm{c}, 0)[\eta_{\lambda_\mathrm{c}}], h\rangle = 0.\end{aligned}$$

However, we know that $\mu'(\lambda_\mathrm{c}) < 0$ by Lemma 5.4. Therefore, we have a contradiction and (5.8) does not hold. Thus, all the assumptions of Crandall and Rabinowitz's theorem [31, Theorem 1.7] are satisfied. Our theorem now follows directly by Crandall and Rabinowitz's result; the smoothness of the maps $t \mapsto \lambda(t)$, $t \mapsto h_t$ follows by [31, Theorem 1.18]. ☐

COROLLARY 5.6. *The OR LdG critical point* $\mathbf{Q}_\mathrm{s}$ *(see Lemma 4.6) is unstable for* $\lambda > \lambda_\mathrm{c}$.

Proof. Consider a perturbation of the form

$$\mathbf{V} := \eta\left(\mathbf{n}_1 \otimes \mathbf{n}_1 - \mathbf{n}_2 \otimes \mathbf{n}_2\right). \tag{5.9}$$

A standard computation shows that the second variation of the LdG energy about the critical point $\mathbf{Q}_\mathrm{s}$ reduces to

$$\delta^2 I[\mathbf{V}] = \int_\Omega \left\{ |\nabla\eta|^2 + \frac{\lambda^2}{L}\left(6Cq_{\mathrm{s},\lambda}^2 - \frac{B^2}{2C}\right)\eta^2 \right\} \mathrm{dA}. \tag{5.10}$$

From Theorem 5.1 and Lemma 5.4, for any $\lambda > \lambda_\mathrm{c}$, there exists an admissible η (vanishing on $\partial\Omega$) such that $\delta^2 I[\mathbf{V}] < 0$ in (5.10). The conclusion now follows. ☐

6. Numerics. In this section, we perform some numerical experiments to study OR solutions on two specific two-dimensional regular polygons — the square and a hexagon, the latter serving to partially illustrate the generic nature of such solutions. We work with the gradient flow model for nematodynamics in the LdG framework, as this is arguably the simplest model to study the evolution of solutions without any external effects or fluid flow. Informally speaking, gradient flow models are dictated by the principle that dynamic solutions evolve along a path of decreasing energy, converging to a stable equilibrium for long times [33]. We adopt the standard gradient flow model associated with the LdG energy

$$\gamma\frac{\partial\mathbf{Q}}{\partial t} = L\Delta\mathbf{Q} - A\mathbf{Q} + B\left(\mathbf{Q}\mathbf{Q} - \frac{|\mathbf{Q}|^2}{3}\mathbf{I}\right) - C|\mathbf{Q}|^2\mathbf{Q} \tag{6.1}$$

where γ is a positive rotational viscosity, $\mathbf{I}$ is the 3×3 identity matrix and $A = -\frac{B^2}{3C}$ so that we can make comparisons between the numerics and the analysis above.
We adopt the same scalings as in [34] i.e. non-dimensionalize the system by setting $\bar{t} := \frac{20tL}{\gamma\lambda^2}, \bar{\mathbf{r}} := \frac{\mathbf{r}}{\lambda}$ where λ is a characteristic geometrical length scale to get

$$\frac{\partial\mathbf{Q}}{\partial\bar{t}} = \bar{\Delta}\mathbf{Q} - \frac{\lambda^2}{L}\left(A\mathbf{Q} - B\left(\mathbf{Q}\mathbf{Q} - \frac{|\mathbf{Q}|^2}{3}\mathbf{I}\right) + C|\mathbf{Q}|^2\mathbf{Q}\right) \tag{6.2}$$

and we drop the bars from all subsequent discussion for brevity.

6.1. Numerics on a square. We first take a re-scaled square centered at the origin with vertices at $(-1,\,-1), (-1,\,1), (1,\,-1), (1,\,1)$ respectively (the original square has edge length 2λ) and impose a boundary condition of the form

$$\mathbf{Q}_{\rm b} = q\,(\hat{\mathbf{x}}\otimes\hat{\mathbf{x}} - \hat{\mathbf{y}}\otimes\hat{\mathbf{y}}) - \frac{B}{6C}\,(2\hat{\mathbf{z}}\otimes\hat{\mathbf{z}} - \hat{\mathbf{x}}\otimes\hat{\mathbf{x}} - \hat{\mathbf{y}}\otimes\hat{\mathbf{y}}) \tag{6.3}$$

where $\hat{\mathbf{x}}$, $\hat{\mathbf{y}}$, $\hat{\mathbf{z}}$ are unit-vectors in the x, y and z-directions respectively and

$$\begin{aligned} &q(x,\,-1) = q(x,\,1) = \frac{B}{2C} && \text{for } -1+\varepsilon \le x \le 1-\varepsilon \\ &q(x,\,-1) = q(x,\,1) = f(x) && \text{otherwise} \\ &q(-1,\,y) = q(1,\,y) = -\frac{B}{2C} && \text{for } -1+\varepsilon \le y \le 1-\varepsilon \\ &q(-1,\,y) = q(1,\,y) = -f(y) && \text{otherwise,} \end{aligned} \tag{6.4}$$

where $f(s) := \frac{B}{2C}\left[\frac{1-|s|}{\varepsilon}\right]$ for $1-\varepsilon \le |s| \le 1$. Consequently, q is fixed to be zero at the vertices. We work with a fixed initial condition of the form (6.3) with

$$\mathbf{Q}_0 := q_0\,(\hat{\mathbf{x}}\otimes\hat{\mathbf{x}} - \hat{\mathbf{y}}\otimes\hat{\mathbf{y}}) - \frac{B}{6C}\,(2\hat{\mathbf{z}}\otimes\hat{\mathbf{z}} - \hat{\mathbf{x}}\otimes\hat{\mathbf{x}} - \hat{\mathbf{y}}\otimes\hat{\mathbf{y}}) \tag{6.5}$$

and

$$q_0(x,\,y) := \begin{cases} \dfrac{B}{2C} & \text{for } -|y| < x < |y| \\ -\dfrac{B}{2C} & \text{for } -|x| < y < |x|, \end{cases} \tag{6.6}$$

and $q_0 = 0$ on the diagonals $x = \pm y$. In other words, $\mathbf{Q}_0$ mimics the OR LdG critical point studied above in the sense that it has a constant eigenframe with an uniaxial cross, with negative order parameter, that connects the four square vertices.
For a boundary condition and an initial condition of the form (6.3)–(6.6), there is a dynamic solution, $\mathbf{Q}(\mathbf{r},\,t)$, of the system (6.2) given by

$$\mathbf{Q}(\mathbf{r},\,t) := q(x,\,y,\,t)\,(\hat{\mathbf{x}}\otimes\hat{\mathbf{x}} - \hat{\mathbf{y}}\otimes\hat{\mathbf{y}}) - \frac{B}{6C}\,(2\hat{\mathbf{z}}\otimes\hat{\mathbf{z}} - \hat{\mathbf{x}}\otimes\hat{\mathbf{x}} - \hat{\mathbf{y}}\otimes\hat{\mathbf{y}}) \tag{6.7}$$

where the evolution of q is governed by

$$\frac{\partial q}{\partial t} = \Delta q - \frac{2C\lambda^2}{L} q\left(q - \frac{B}{2C}\right)\left(q + \frac{B}{2C}\right). \tag{6.8}$$

In what follows, we solve the evolution equation (6.8) on a re-scaled square for different values of λ. We use a standard finite-difference method for the spatial derivatives and the Runge-Kutta scheme for time-stepping in the numerical simulations (also see [34] for more discussion on numerical methods). We expect to see $q = 0$ along $x = \pm y$ for small values of λ, since the OR solution is the unique LdG critical point for small λ and transition layers near a pair of opposite edges for large λ.
Let $\bar{\lambda}^2 := \frac{2C\lambda^2}{L}$ and as in [21], we take $B = 0.64\times 10^4 \mathrm{Nm}^{-2}$, $C = 0.35\times 10^4 \mathrm{Nm}^{-2}$ throughout this section. Recall that at a fixed temperature, the bare biaxial correlation length, $\xi \propto \sqrt{\frac{LC}{B^2}}$ and since B and C are comparable for our simulations, ξ and

the length scale, $\sqrt{\frac{L}{C}}$, are of the same order of magnitude. In Figures 6.1, 6.2, we solve (6.8), subject to (6.4) and the initial condition, $q(x,\, y,\, 0) = q_0(x,\, y)$ where q_0 is defined in (6.6), for $\bar{\lambda}^2 = 0.05$ and $\bar{\lambda}^2 = 200$ respectively. For $\bar{\lambda}^2 = 0.05$, the scalar profile relaxes the initial sharp transition layers at $x = \pm y$ but retains the vanishing diagonal cross with $q(x, \pm x, t) = 0$ for all times. The corresponding dynamic solution, $\mathbf{Q}(\mathbf{r}, t)$ in (6.7), has an uniaxial cross with negative order parameter, connecting the four square vertices, consistent with the stability and uniqueness results for the LdG OR solution in Sections 4 and 5. For $\bar{\lambda}^2 = 200$, the initial condition has the diagonal cross but the diagonal cross rapidly relaxes into a pair of transition layers, one layer being localized near $x = -1$ (or $y = -1$) and the other layer being localized near $x = +1$ (or $y = +1$); see Figure 6.2. In Figure 6.3, we plot $q(0,\, 0)$ — the value of the converged solution at the origin as a function of $\bar{\lambda}^2$. We have lost the diagonal cross if $q(0,\, 0) \neq 0$ and hence, one might reasonably deduce that the OR solution loses stability for values of $\bar{\lambda}^2$ for which $q(0,\, 0) \neq 0$. In Figure 6.3, we see that $q(0,\, 0) = 0$ for $\bar{\lambda}^2 \leq 9.2$ and $q(0,\, 0) \neq 0$ for $\bar{\lambda}^2 > 9.2$ (in terms of the original variables, $\lambda^2 > 4.6\frac{L}{C}$) and the picture is consistent with a supercritical pitchfork bifurcation as established in Theorem 5.1.

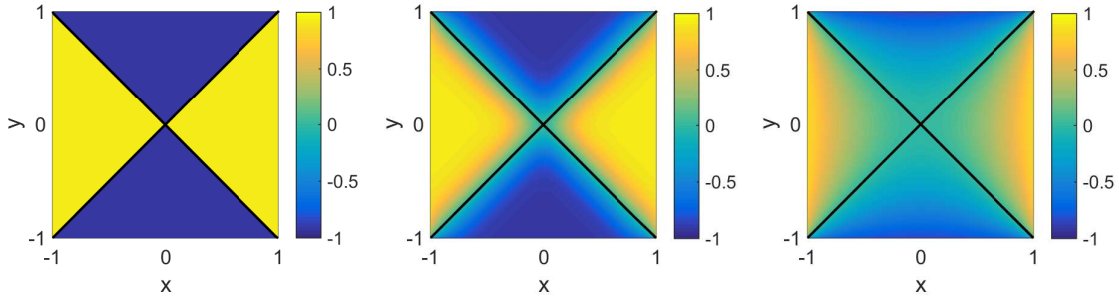

Figure 6.1: $q(x,\, y,\, t)$ for $t = 0$, $t = 0.01$ and $t = 2$ for $\bar{\lambda}^2 = 0.05$.

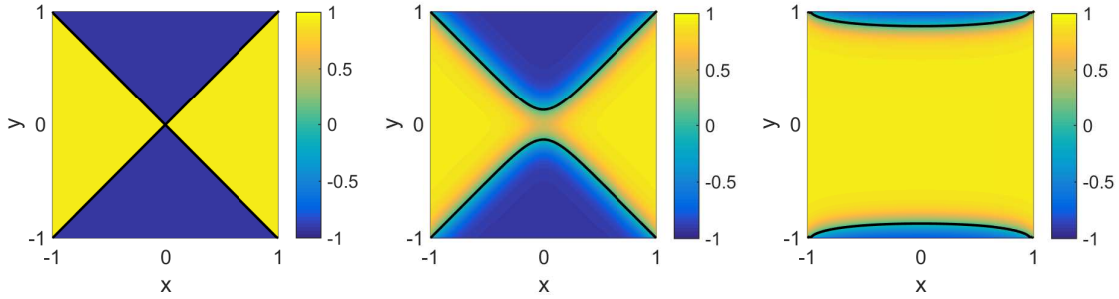

Figure 6.2: $q(x,\, y,\, t)$ for $t = 0$, $t = 0.5$ and $t = 2$ for $\bar{\lambda}^2 = 200$.

6.2. Order Reconstruction on a Hexagon: Analysis and Numerics. In this section, we look for OR type solutions on a regular hexagon, of edge length λ, at the fixed temperature, $A = -\frac{B^2}{3C}$ as before. We interpret OR solutions loosely i.e.

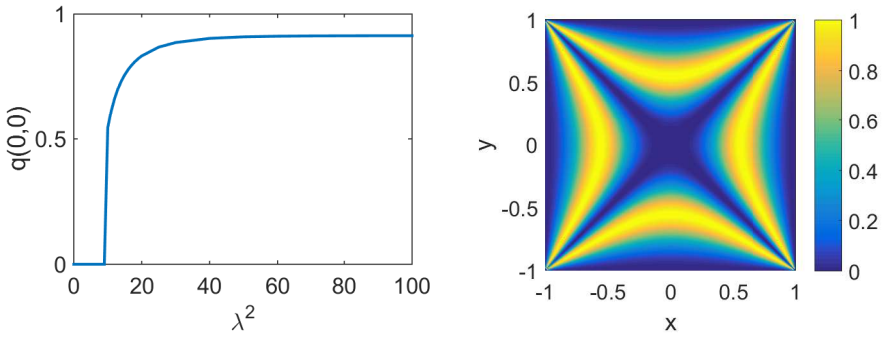

Figure 6.3: Left: $q(0,0)$ for the steady solution as $\bar{\lambda}^2$ varies, the critical value is $\bar{\lambda}^2 = 9.2$. Right: plot of the biaxiality parameter β^2 (see Equation (6.19)) for $\bar{\lambda}^2 = 0.35 \times 10^{-2}$ and $t = 2$.

we look for critical points of the LdG energy which have an interior ring of maximal biaxiality inside the hexagon. Let H be a regular re-scaled hexagon, centered at the origin with vertices $(1,\,0)$, $(1/2,\,\sqrt{3}/2)$, $(-1/2,\,\sqrt{3}/2)$, $(-1,\,0)$, $(-1/2,\,-\sqrt{3}/2)$, $(1/2,\,-\sqrt{3}/2)$. We take our domain Ω to be the set of points $(x,\,y)$ in the interior of H that satisfy the inequalities

$$|x| < 1-\varepsilon, \quad \frac{1}{2}\left|x+\sqrt{3}y\right| < 1-\varepsilon, \quad \frac{1}{2}\left|x-\sqrt{3}y\right| < 1-\varepsilon.$$

The domain Ω is a truncated hexagon (see Figure 3.1) and has the same set of symmetries as the original hexagon H, that is,

$$\{S \in \mathrm{O}(2)\colon S\Omega \subseteq \Omega\} = \{S \in \mathrm{O}(2)\colon SH \subseteq H\} =: D_6. \tag{6.9}$$

The set of symmetries D_6 consists of six reflection symmetries about the symmetry axes of the hexagon, and six rotations of angles $k\pi/3$ for $k \in \{0,\,\ldots,\,5\}$. We label the "long" edges counterclockwise, that is the edges common to both $\partial\Omega$ and ∂H, as $C_1,\,\ldots,\,C_6$, starting from $(1,\,0)$. We impose Dirichlet boundary conditions

$$\mathbf{Q}(\mathbf{r}) = \mathbf{Q}_{\mathrm{b}}(\mathbf{r}) := \frac{B}{C}\left(\mathbf{n}_{\mathrm{b}}(\mathbf{r}) \otimes \mathbf{n}_{\mathrm{b}}(\mathbf{r}) - \frac{\mathbf{I}}{3}\right), \tag{6.10}$$

on the C_i's, where $\mathbf{n}_{\mathrm{b}}$ is a tangent unit vector field to ∂H, i.e.

$$\mathbf{n}_{\mathrm{b}}(\mathbf{r}) := \begin{cases} (-1/2,\,\sqrt{3}/2,\,0) & \text{if } \mathbf{r} \in C_1 \cup C_4 \\ (-1,\,0,\,0) & \text{if } \mathbf{r} \in C_2 \cup C_5 \\ (-1/2,\,-\sqrt{3}/2,\,0) & \text{if } \mathbf{r} \in C_3 \cup C_6. \end{cases} \tag{6.11}$$

We also impose Dirichlet conditions on the "short" edges of $\partial\Omega$. For instance, on the short edge connecting the vertices $(1-\varepsilon,\,\sqrt{3}\varepsilon)$, $(1-\varepsilon,\,-\sqrt{3}\varepsilon)$, we fix

$$\mathbf{Q}_{\mathrm{b}}(x,\,y) := \frac{B}{C}\left(\mathbf{n}_{\mathrm{b}}(x,\,y) \otimes \mathbf{n}_{\mathrm{b}}(x,\,y) - \frac{\mathbf{I}}{3}\right)$$

for $\mathbf{n}_{\mathrm{b}}(x,\,y) := \frac{2\varepsilon}{\sqrt{\varepsilon^2+y^2}}\left(-\frac{1}{2},\,\frac{y}{2\varepsilon},\,0\right)$. We extend the boundary datum $\mathbf{Q}_{\mathrm{b}}$ to the other short edges by successive rotations of $\pi/3$. By construction, the boundary datum is consistent with the symmetries of the hexagon.

We look for critical points of the LdG energy (2.3) on Ω, such that (i) the corresponding $\mathbf{Q}$-tensor has $\hat{\mathbf{z}}$ as an eigenvector with constant eigenvalue $-\frac{B}{3C}$, and (ii) the origin is a uniaxial point with negative scalar order parameter. The long edges are subject to a uniaxial Dirichlet condition with positive order parameter (see (6.10) and (6.11)) and it is reasonable to expect a ring of maximal biaxiality separating the central uniaxial point with negative order parameter from the positively ordered uniaxial Dirichlet conditions, as will be corroborated by the numerics below.
As in the case of a square, we briefly comment on our choice of the boundary conditions on a hexagon. Our analytical and numerical results will extend to three-dimensional wells with a hexagonal cross-section, Dirichlet conditions of the form (6.10) on the lateral surfaces and free boundary conditions on the top and bottom surfaces. Of course, there may be other more physically relevant choices of the boundary conditions that might yield more exotic profiles with more complicated defect structures, especially near the hexagon vertices. We focus on this particular choice since it is an immediate generalization of the conditions used on a square domain and renders itself to easy comparison.
In view of (i), we look for critical points of the form

$$\mathbf{Q}(\mathbf{r}) = \left(\begin{array}{cc|c} & & 0 \\ \multicolumn{2}{c|}{\mathbf{P}(\mathbf{r}) + \frac{B}{6C}\mathbf{I}_2} & 0 \\ \hline 0 & 0 & -B/3C \end{array}\right), \tag{6.12}$$

where $\mathbf{P}(\mathbf{r})$ is a 2×2, symmetric and traceless matrix (in the space $S_0^{2\times 2}$) and $\mathbf{I}_2$ is the 2×2 identity matrix. The condition (ii) is satisfied if $\mathbf{P}(0,\, 0) = 0$. By substitution, we see that $\mathbf{Q}$ is a LdG critical point of (2.3) if $\mathbf{P}$ is a solution of the system

$$\Delta\mathbf{P} = \frac{\lambda^2}{L}\left\{-\frac{B^2}{2C}\mathbf{P} - B\left(\mathbf{P}\mathbf{P} - \frac{\mathbf{I}_2}{2}|\mathbf{P}|^2\right) - C|\mathbf{P}|^2\mathbf{P}\right\} \tag{6.13}$$

or, equivalently, a critical point of the functional

$$F[\mathbf{P}] := \int_\Omega \left\{\frac{1}{2}\,|\nabla\mathbf{P}|^2 + \frac{\lambda^2}{L}\left(-\frac{B^2}{4C}\,\mathrm{tr}\,\mathbf{P}^2 - \frac{B}{3}\,\mathrm{tr}\,\mathbf{P}^3 + \frac{C}{4}(\mathrm{tr}\,\mathbf{P}^2)^2\right)\right\}\,\mathrm{dA}. \tag{6.14}$$

Let $\mathbf{P}_\mathrm{b}$ denote the boundary datum for $\mathbf{P}$, related to $\mathbf{Q}_\mathrm{b}$ via (6.12).
LEMMA 6.1. *For any $\lambda > 0$, there exists a critical point $\mathbf{P}_\mathrm{s} \in C^2(\Omega)\cap C^0(\overline{\Omega})$ of (6.14) which satisfy the boundary condition $\mathbf{P}_\mathrm{s} = \mathbf{P}_\mathrm{b}$ on $\partial\Omega$ and $\mathbf{P}_\mathrm{s}(0,\, 0) = 0$.*
The corresponding $\mathbf{Q}$-tensor, denoted by $\mathbf{Q}_\mathrm{s}$, is then related to $\mathbf{P}_\mathrm{s}$ via (6.12), and is a critical point of the LdG energy (by construction).
Proof of Lemma 6.1. Let $\mathscr{A}$ be the class of admissible configurations, i.e. maps $\mathbf{P} \in W^{1,2}(\Omega,\, S_0^{2\times 2})$ that satisfies $\mathbf{P} = \mathbf{P}_\mathrm{b}$ on $\partial\Omega$. Let $\mathscr{A}_\mathrm{sym}$ be the class of admissible configurations that are consistent with the symmetries of the hexagon i.e. $\mathscr{A}_\mathrm{sym}$ is the set of maps $\mathbf{P} \in \mathscr{A}$ that satisfy

$$\mathbf{P}(\mathbf{r}) = S\mathbf{P}(S^\mathsf{T}\mathbf{r})S^\mathsf{T} \tag{6.15}$$

for a.e. $\mathbf{r} \in \Omega$ and any matrix $S \in D_6$ where D_6 is defined in (6.9).Recall that the boundary datum $\mathbf{P}_\mathrm{b}$ satisfies (6.15) by construction, so the set $\mathscr{A}_\mathrm{sym}$ is non-empty. We can prove the existence of a minimiser $\mathbf{P}_\mathrm{s} \in \mathscr{A}_\mathrm{sym}$ for the energy F given by (6.14), by the direct methods in the calculus of variations.
Clearly, $\mathbf{P}_\mathrm{s}$ is a critical point for F restricted to $\mathscr{A}_\mathrm{sym}$, but we do not know if it is a critical point for F in $\mathscr{A}$, hence a solution of the Euler-Lagrange system (6.13).

However, the right-hand side of (6.15) defines an isometric action of D_6 on $\mathscr{A}$, and the energy F is invariant with respect to this action. Therefore, we can apply Palais' principle of symmetric criticality [20, Theorem p. 23] to conclude that critical points of F in the restricted space $\mathscr{A}_{\text{sym}}$ exist as critical points in $\mathscr{A}$. We conclude that $\mathbf{P}_{\text{s}}$ is a critical point of F in $\mathscr{A}$, i.e. a solution of (6.13). By elliptic regularity, we obtain that $\mathbf{P}_{\text{s}} \in C^2(\Omega) \cap C^0(\overline{\Omega})$. Finally, we evaluate (6.15) at $\mathbf{r} = (0, 0)$ to obtain that

$$\mathbf{P}(0, 0) = S\mathbf{P}(0, 0)S^{\mathsf{T}} \qquad \text{for any } S \in D_6,$$

which necessarily requires that $\mathbf{P}_{\text{s}}(0, 0) = 0$ as stated. □

Next, we perform numerical experiments on the regular re-scaled hexagon H (not truncated hexagon), with the gradient flow model (6.2), to investigate the stability of the OR-type critical point constructed in Lemma 6.1. We solve the system for Q_{ij}, $i, j = 1, 2, 3$ in (6.2) with different values of $\bar{\lambda}^2 := \frac{C\lambda^2}{L}$, at $A = -\frac{B^2}{3C}$.

We impose Dirichlet conditions on all six edges of the form

$$\mathbf{Q}_{\text{b}}(x, y) = \frac{B}{C}\left(\mathbf{n}_{\text{b}} \otimes \mathbf{n}_{\text{b}} - \frac{\mathbf{I}}{3}\right) \tag{6.16}$$

and there are discontinuities at the vertices. The choice of $\mathbf{n}_{\text{b}}$ is dictated by the tangent unit-vector to the edge in question i.e. see (6.11), and at a given vertex, we fix $\mathbf{Q}_{\text{b}}$ to be the average of the two intersecting edges. We impose an initial condition which divides the hexagon into six regions, which are three alternating constant uniaxial states, as shown in Figure 6.4. This initial condition is not defined at the origin but this does not pose to be a problem for the numerics. We look for solutions which have $\hat{\mathbf{z}}$ as an eigenvector and have a uniaxial point at the origin with negative order parameter. This translates to (i) $Q_{33} = -\frac{B}{3C}$ everywhere, (ii) $Q_{13} = Q_{23} = 0$ everywhere, (ii) $Q_{11} = Q_{22} = \frac{B}{6C}$ and $Q_{12} = 0$ at the origin.

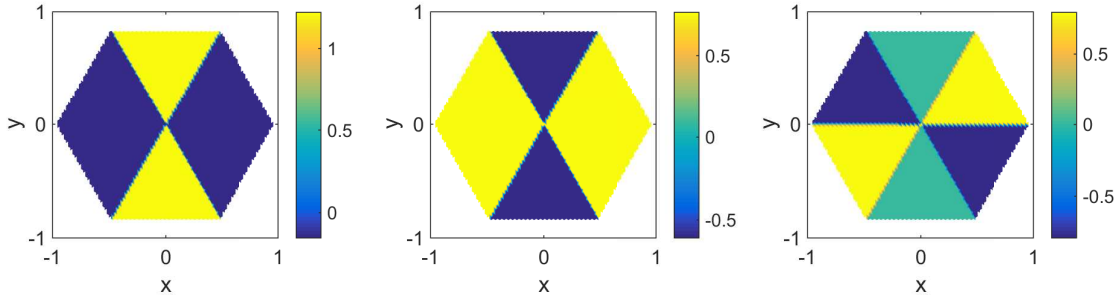

Figure 6.4: Q_{11}, Q_{22} and Q_{12} for $t = 0$.

We solve the gradient-flow system on H with $\bar{\lambda}^2 = 10^{-6}$, with the fixed Dirichlet condition and initial condition as described above. In Figures 6.5 we plot Q_{12}, Q_{11}, Q_{22} of the converged solution and see that the origin is indeed an uniaxial point with negative scalar order parameter i.e. the dynamic solution at the origin,

$$\mathbf{Q}(0, 0, t) = -\frac{B}{2C}\left(\hat{\mathbf{z}} \otimes \hat{\mathbf{z}} - \frac{\mathbf{I}}{3}\right) \tag{6.17}$$

for large times. Further, we numerically verify that

$$Q_{33}(\mathbf{r}, t) = -\frac{B}{3C}, \qquad Q_{13}(\mathbf{r}, t) = Q_{23}(\mathbf{r}, t) = 0 \tag{6.18}$$

for all times t, so that $\hat{\mathbf{z}}$ is indeed an eigenvector with constant eigenvalue.
In Figure 6.7, we plot the biaxiality parameter, β^2, of the converged solution

$$\beta^2 = 1 - 6\frac{\left(\mathrm{tr}\mathbf{Q}^3\right)^2}{\left(\mathrm{tr}\,\mathbf{Q}^2\right)^3} \in [0,1] \tag{6.19}$$

at $\bar{\lambda}^2 = 10^{-6}$ and see a distinct ring of maximal biaxiality (with $\beta^2 = 1$ such that $\mathbf{Q}$ has a zero eigenvalue) around the origin, hence yielding an OR-type solution on H. (Note that the biaxiality parameter, β^2, is well-defined for $\mathrm{tr}\,\mathbf{Q}^2 \neq 0$, i.e. $\mathbf{Q} \neq 0$ and we set $\beta^2 = 0$ for $\mathbf{Q} = 0$ by definition.)
In Figures 6.6, 6.7 we plot the components of the converged solutions at the origin as a function of $\bar{\lambda}^2$. We see that (6.18) holds for all $\bar{\lambda}^2$ so that $\hat{\mathbf{z}}$ is always an eigenvector. Further, the converged solution respects $Q_{12} = 0, Q_{11} = Q_{22} = \frac{B}{6C}$ at the origin for $\bar{\lambda}^2 \leq 7$ and hence, we have an uniaxial point with negative order parameter at the origin for $\bar{\lambda}^2 \leq 7$. On these grounds, we expect that the OR-type solution is locally stable on H, for $\lambda^2 < 7\frac{L}{C}$.As λ increases, we find that the solution is predominantly uniaxial everywhere inside the hexagon with positive order parameter and regions of maximal biaxiality and uniaxial points of negative order parameter migrate to a pair of opposite vertices. We have not explored the regime of large λ carefully in this paper. The qualitative trends are the same as those on a regular square.

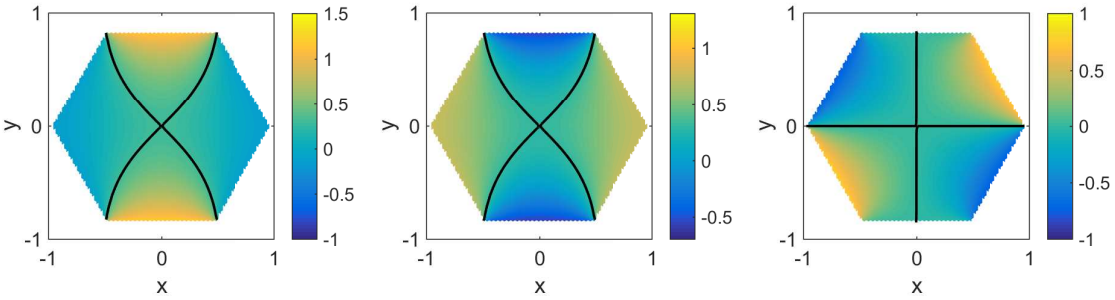

Figure 6.5: Q_{11} and Q_{22} with contours at level $\frac{B}{6C}$ and Q_{12} with contours at level 0 for $\bar{\lambda}^2 = 10^{-6}$ and $t = 2$.

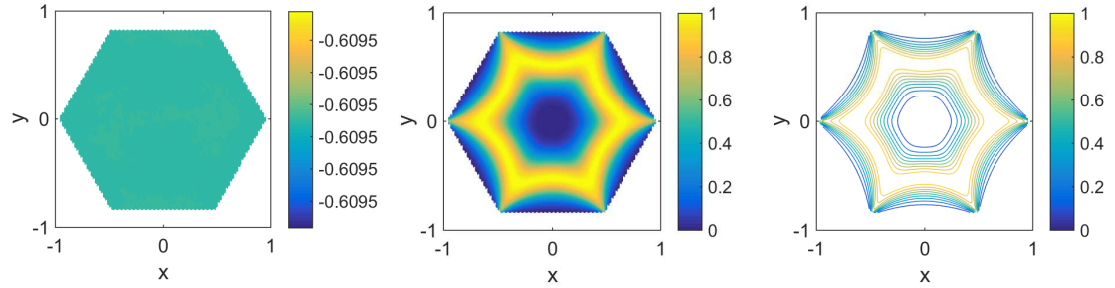

Figure 6.6: Left: $Q_{33} = -Q_{11} - Q_{22}$ for $\bar{\lambda}^2 = 10^{-6}$ and $t = 2$. Center and right: plot and contour plot of biaxiality parameter β^2 for $\bar{\lambda}^2 = 10^{-6}$ and $t = 2$.

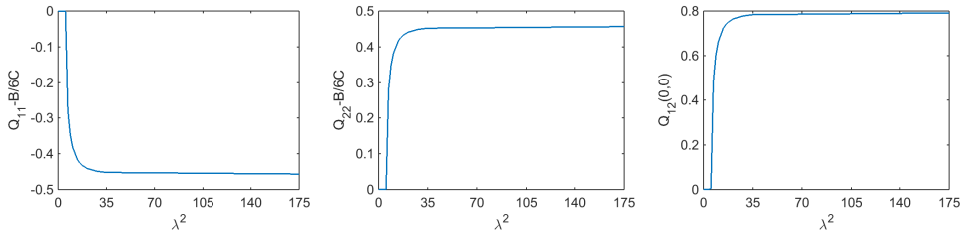

Figure 6.7: $Q_{11} - \frac{B}{6C}$, $Q_{22} - \frac{B}{6C}$, Q_{12} at the origin for various $\bar{\lambda}$. The critical value of $\bar{\lambda}^2 = 7$.

7. Conclusions. We analytically and numerically study an OR-type LdG critical point on a square domain at a fixed temperature, motivated by the WORS critical point reported in [1] distinguished by a uniaxial cross with negative order parameter along the square diagonals. The LdG OR critical point is globally stable for edge lengths comparable to the length scale, $\sqrt{\frac{LC}{B^2}}$. The LdG critical point loses stability as λ increases and undergoes a supercritical pitchfork bifurcation as λ increases in a reduced scalar setting. In the scalar framework, the LdG OR-type critical point loses stability with respect to LdG critical points that tend to have transition layers localized near the square edges. Whilst this is enough to rigorously prove instability of the LdG OR-type critical point in the full LdG framework (with the full five degrees of freedom), we expect the bifurcation picture to be more complicated in the full LdG setting. Further, our preliminary numerical investigations on a square and a hexagon suggest that OR-type critical points exist and are globally stable for regular two-dimensional polygons with an even number of sides, when the side length is sufficiently small. Of course, the interpretation of an OR-type critical point does vary from geometry to geometry and hence, one cannot make a direct comparison between the stability criteria but only comment on qualitative trends. We will study the generic character of OR-type critical points in future work.

8. Acknowledgements. G.C. has received funding from the European Research Council under the European Union's Seventh Framework Programme (FP7/2007-2013) / ERC grant agreement n° 291053. A.M. is supported by an EPSRC Career Acceleration Fellowship EP/J001686/1 and EP/J001686/2 and an OCIAM Visiting Fellowship. A.S. is supported by an Engineering and Physical Sciences Research Council (EPSRC) studentship.

REFERENCES

[1] S. Kralj and A. Majumdar. Order reconstruction patterns in nematic liquid crystal wells. *Proc. R. Soc. Lond. Ser. A Math. Phys. Eng. Sci.*, 470(2169):20140276, 18, 2014.
[2] P. G. De Gennes and J. Prost. *The Physics of Liquid Crystals*. Clarendon Press, Oxford, 1974.
[3] E. G. Virga. *Variational Theories for Liquid Crystals*, volume 8 of *Applied Mathematics and Mathematical Computation*. Chapman & Hall, London, 1994.
[4] C. Tsakonas, A. J. Davidson, C. V. Brown, and N. J. Mottram. Multistable alignment states in nematic liquid crystal filled wells. *Appl. Phys. Lett.*, 90(11):111913, 2007.
[5] C. Anquetil-Deck, D. J. Cleaver, and T. J. Atherton. Competing alignments of nematic liquid crystals on square-patterned substrates. *Phys. Rev. E*, 86:041707, Oct 2012.
[6] C. Luo, A. Majumdar, and R. Erban. Multistability in planar liquid crystal wells. *Phys. Rev. E*, 85:061702, Jun 2012.

[7] A. Lewis, I. Garlea, J. Alvarado, O. Dammone, O. Howell, A. Majumdar, B. Mulder, M. P. Lettinga, G. Koenderink, and D. Aarts. Colloidal liquid crystals in rectangular confinement: Theory and experiment. *Soft Matter*, 39(10):7865–7873, October 2014.

[8] N. Schopohl and T. J. Sluckin. Defect core structure in nematic liquid crystals. *Phys. Rev. Lett.*, 59:2582–2584, 1987.

[9] E. Penzenstadler and H.-R. Trebin. Fine structure of point defects and soliton decay in nematic liquid crystals. *J. Phys. (Paris)*, 50(9):1989, 1027–1040.

[10] S. Mkaddem and E. C. Gartland. Fine structure of defects in radial nematic droplets. *Phys. Rev. E*, 62:6694–6705, Nov 2000.

[11] P. Palffy-Muhoray, E. C. Gartland, and J.-R. Kelly. A new configurational transition in inhomogeneous nematics. *Liq. Cryst.*, 16(4):713–718, 1994.

[12] F. Bisi, E. C. Gartland, R. Rosso, and E. G. Virga. Order reconstruction in frustrated nematic twist cells. *Phys. Rev. E*, 68:021707, Aug 2003.

[13] F. Bisi, E. G. Virga, and G. E. Durand. Nanomechanics of order reconstruction in nematic liquid crystals. *Phys. Rev. E*, 70:042701, Oct 2004.

[14] X. Lamy. Bifurcation analysis in a frustrated nematic cell. *J. Nonlinear Sci.*, 24(6):1197–1230, 2014.

[15] X. Zhou, Z. Zhang, Q. Zhang, and W. Ye. Order reconstruction in a nanoconfined nematic liquid crystal between two coaxial cylinder. *Materials*, 8(12):8072–8086, 2015.

[16] D. Golovaty, J. A. Montero, and P. J. Sternberg. Dimension reduction for the Landau-de Gennes model in planar nematic thin films. *J Nonlinear Sci*, 25:1431–1451, 2015.

[17] H. Dang, P. C. Fife, and L. A. Peletier. Saddle solutions of the bistable diffusion equation. *Z. Angew. Math. Phys.*, 43(6):984–998, 1992.

[18] M. Schatzman. On the stability of the saddle solution of Allen-Cahn's equation. *Proc. Roy. Soc. Edinburgh Sect. A*, 125(6):1241–1275, 1995.

[19] M. Robinson, C. Luo, A. Majumdar, and R. Radek Erban. From molecular to continuum modelling of bistable liquid crystal devices. In preparation, 2016.

[20] R. S. Palais. The principle of symmetric criticality. *Comm. Math. Phys.*, 69(1):19–30, 1979.

[21] N. J. Mottram and C. Newton. Introduction to Q-tensor theory. Technical Report 10, Department of Mathematics, University of Strathclyde, 2004.

[22] A. Majumdar. Equilibrium order parameters of nematic liquid crystals in the Landau-de Gennes theory. *Eur. J. Appl. Math.*, 21(2):181–203, 2010.

[23] L. C. Evans. *Partial Differential Equations*, volume 19 of *Graduate Studies in Mathematics*. American Mathematical Society, Providence, RI, second edition, 2010.

[24] A. Majumdar and A. Zarnescu. Landau-De Gennes theory of nematic liquid crystals: the Oseen-Frank limit and beyond. *Arch. Ration. Mech. Anal.*, 196(1):227–280, 2010.

[25] L. Modica and S. Mortola. Il limite nella Γ-convergenza di una famiglia di funzionali ellittici. *Boll. Un. Mat. Ital. A (5)*, 14(3):526–529, 1977.

[26] P. Sternberg. The effect of a singular perturbation on nonconvex variational problems. *Arch. Rational Mech. Anal.*, 101(3):209–260, 1988.

[27] A. Braides. A handbook of Γ-convergence. volume 3 of *Handbook of Differential Equations: Stationary Partial Differential Equations*, pages 101–213. North-Holland, 2006.

[28] P. Grisvard. *Elliptic problems in nonsmooth domains*, volume 24 of *Monographs and Studies in Mathematics*. Pitman (Advanced Publishing Program), Boston, MA, 1985.

[29] D. Gilbarg and N. S. Trudinger. *Elliptic partial differential equations of second order*. Classics in Mathematics. Springer-Verlag, Berlin, 2001. Reprint of the 1998 edition.

[30] F. Bethuel, H. Brezis, and F. Hélein. Asymptotics for the minimization of a Ginzburg-Landau functional. *Calc. Var. Partial Dif.*, 1(2):123–148, 1993.

[31] M. G. Crandall and P. H. Rabinowitz. Bifurcation from simple eigenvalues. *J. Functional Analysis*, 8:321–340, 1971.

[32] M. G. Crandall and P. H. Rabinowitz. Bifurcation, perturbation of simple eigenvalues and linearized stability. *Arch. Rational Mech. Anal.*, 52:161–180, 1973.

[33] M. A. Peletier. Energies, gradient flows, and large deviations: a modelling point of view. Lecture notes, Università di Pisa, 2011. http://www.win.tue.nl/ mpeletie/Onderwijs/Pisa2011/PeletierLectureNotesPisa2011.pdf

[34] A. Majumdar, P. A. Milewski, and A. Spicer. Front Propagation at the Nematic-Isotropic Transition Temperature. *SIAM J. Appl. Math.*, 76(4), 1296–1320, 2016.